cancers and is widely used as a treatment option for solid cancers (16-18). The use of PDT as a treatment for MPM has been investigated under both clinical and experimental conditions (19-21). Friedberg *et al* reported a phase I clinical trial of Foscan-mediated PDT and surgery in patients with MPM (20). They reported that Foscan-mediated PDT afforded the option of accomplishing tumor debulking using a lung-sparing pleurectom/decortication, rather than EPP. A phase III randomized trial of surgery and chemotherapy with or without intra-operative PDT using the first-generation photosensitizer Photofrin, was reported in 1997 (22). The study concluded that PDT using Photofrin did not prolong patient survival or increase local MPM control. However, we recently reported that PDT using the second-generation photosensitizer NPe6, has a strong antitumor effect against large tumors, which are unsuitable for treatment with Photofrin-PDT (23). NPe6 has a major absorption band at 664 nm, which is longer than the Photofrin band (630 nm), and NPe6-PDT can affect deeper lesions. Therefore, in an attempt to establish a new treatment modality for MPM, we examined the antitumor effect of combination therapy consisting of pemetrexed chemotherapy and NPe6-PDT by comparing the antitumor effects of pemetrexed administered before or after NPe6-PDT in both *in vitro* and *in vivo* models.

Materials and methods

Cell cultures. The human mesothelioma cell lines, H28, H2452, MSTO-211H, and H2052 were purchased from the American Type Culture Collection (ATCC) (Manassas, VA, USA) (24,25). These cell lines and human breast cancer MCF-7 cells transfected with human procaspase-3 cDNA (MCF-7c3 cells) were cultured in RPMI-1640 medium containing 10% fetal bovine serum (26).

Photosensitizer. NPe6 (Meiji Seika Pharma Co., Ltd., Tokyo, Japan) is a second-generation water-soluble photosensitizer with a molecular weight of 799.69 and a chlorine annulus; its highest absorption peak occurs at 407 nm, while a second peak occurs at 664 nm (17,27).

Laser unit. A diode laser (Panasonic Healthcare Co., Ltd., Kanagawa, Japan) emitting continuous wave laser light at a wavelength of 664 nm was used as the light source for the excitation of NPe6 (28).

Measurement of the fluorescence intensity of NPe6 in the cells. MSTO-211H cells were exposed to pemetrexed at an IC_{50} dose of 1.2 μM for 48 h, and then were exposed to NPe6 (15 μg/ml) for 4 h. The cells were washed with phosphate buffered saline (PBS). The NPe6 remaining in the cells was excited at 405 nm, and the fluorescence was detected with a charged coupled device (CCD) camera system (Argus/HiSCa; Hamamatsu Photonics Co. Ltd., Shizuoka, Japan) through a multilaminate interference filter capable of selecting a fluorescence wavelength of 630 nm, as previously reported (29).

Determination of cell viability. We evaluated the growth inhibitory effects using the tetrazolium salt WST-1 assay according to the manufacturer's instructions, as described previously (29,30). The effects of four different treatment schedules were examined. For the treatment of PDT alone, cells were seeded into 96-well microculture plates at a density of $1x10^4$ cells/well and allowed to adhere to the dish overnight. NPe6 was then added to the medium in increasing concentrations, followed by incubation at 37°C in the dark for 24 h. The cells were washed with PBS and the medium was replaced; the cells were then irradiated with a laser (33 mW/cm^2; total energy, 10 J/cm^2) and cell viability was measured 72 h later. For the treatment of PDT followed by pemetrexed, the cells were incubated with NPe6 (10 μg/ml) for 24 h. Then, the cells were treated by PDT and the medium was replaced with a medium containing pemetrexed, followed by culturing for 48 h. For the treatment of pemetrexed alone, the cells were incubated with pemetrexed for 48 h. For the treatment of pemetrexed followed by PDT, the cells were incubated with pemetrexed; 24 h later, NPe6 (10 μg/ml) was added. Forty-eight hours later, the cells were treated by PDT then incubated for 24 h. For each protocol, the cell viability was measured at 72 h after the start of the treatment. Independent experiments were repeated at least three times to confirm the data.

Nude mice. Five-week-old BALB/c nude mice weighing 20-30 g were obtained from the Charles River Laboratories International, Inc. (L'Abresele, France). The animal experiments were conducted in accordance with the guidelines of the Animal Ethics Committee of Tokyo Medical University, complying with the Guidelines for the Welfare and Use of Animals in Cancer Research (31).

Protocol and therapeutic procedures. MSTO-211H cells were washed twice in Hank's solution (Invitrogen Life Technologies, Carlsbad, CA, USA), and 10^7 cells were injected subcutaneously into the right thigh of individual nude mice. Treatments were initiated 7 days after tumor cell implantation, when the MSTO-211H tumors were ~200 mm^3 in volume. The tumor volumes were calculated using the following formula: tumor volume = $LD^2/2$ (L, long diameter; D, short diameter) (32). For the pemetrexed followed by PDT treatment, mice were intraperitoneally injected with pemetrexed (150 mg/kg daily) on days 7-11; on day 12, the mice were intravenously injected with NPe6 (10 mg/kg) and irradiated with a 664-nm laser (100 J/cm^2) 2 h later. The irradiation time was 16 min and 40 sec. For the PDT followed by pemetrexed treatment, mice were intravenously injected with NPe6 (10 mg/kg) and 2 h later irradiated with a 664-nm laser (100 J/cm^2) on day 7; on days 8-12, the mice were intraperitoneally injected with pemetrexed (150 mg/kg daily). The progress of each tumor was measured every day until day 28, and the ratio of the tumor volume was calculated by comparing the volume with the tumor volume on day 7. All the *in vivo* studies were performed in accordance with the Guidelines for the Welfare and Use of Animals in Cancer Research (31).

Immunohistochemical analysis. Cells were grown on glass coverslips in 35-mm petri dishes. To analyze the expression of TS, the coverslips were removed from the petri dishes, washed with PBS, and fixed in 1% formaldehyde for 30 min.

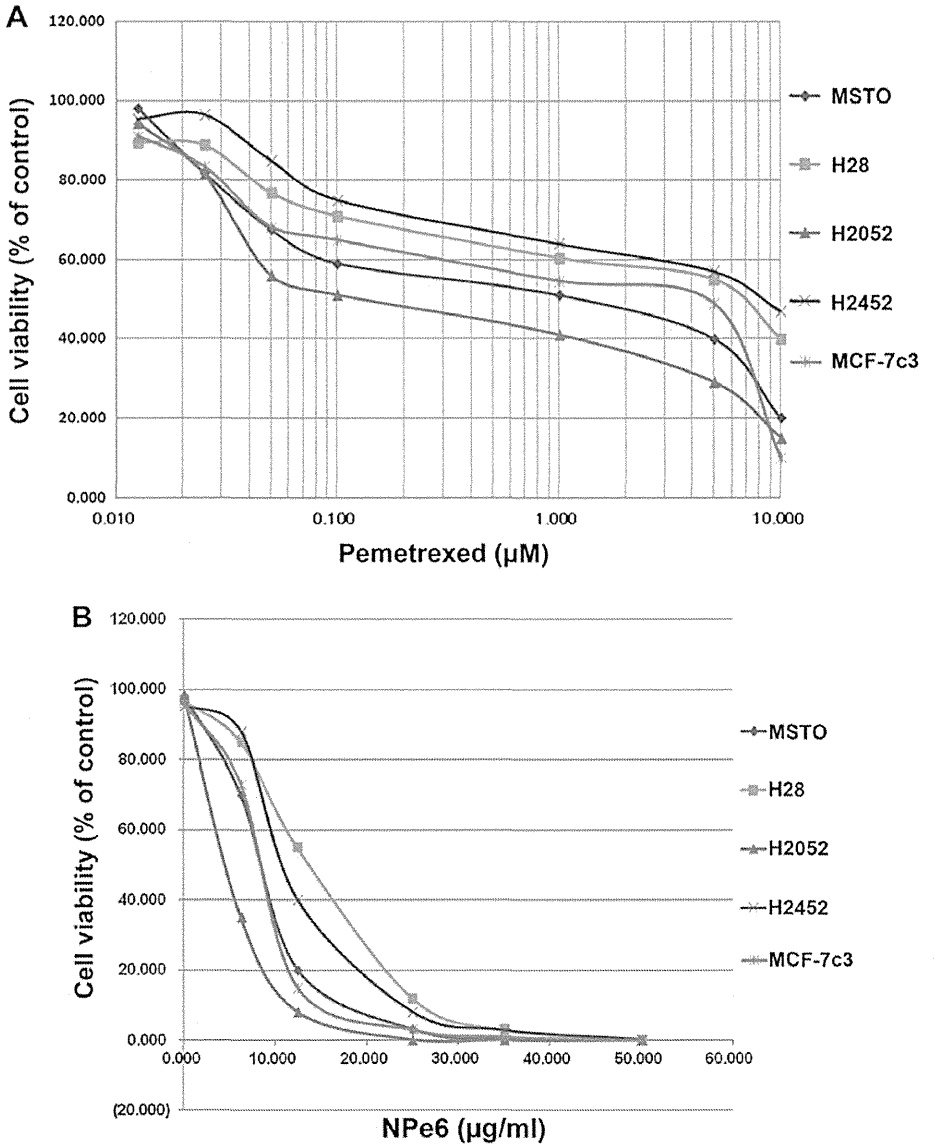

Figure 1. (A) Growth-inhibitory effect of pemetrexed in MSTO-211H (♦), H28 (■), H2052 (▲), H2452 (×), and MCF-7c3 cells (✳). Cells were exposed to pemetrexed for 96 h, and the growth-inhibitory effect was measured using the WST assay. (B) Growth-inhibitory effect of NPe6-PDT in MSTO-211H (♦), H28 (■), H2052 (▲), H2452 (×), and MCF-7c3 cells (✳). Cells were exposed to NPe6 for 24 h and then washed with phosphate buffered saline (PBS); the medium was replaced. The cells were then irradiated with a diode laser (33 mW/cm^2, 10 J/cm^2) and cultured for another 48 h. The growth-inhibitory effect was measured using the WST assay.

After rinsing twice with PBS, the fixed cells were incubated in IFA buffer (PBS containing 1% bovine serum albumin, 0.1% Tween-20) for 10 min and then in IFA-containing mouse anti-TS antibody (clone 8F1; Zymed Laboratories, Inc., San Francisco, CA, USA) for 1 h at room temperature (26,30,32).

The MSTO-211H tumors in BALB/c nude mice were collected before PDT and 24 h after PDT. We performed an immunohistochemical analysis of these samples using anti-TS antibody (clone 8F1; Zymed Laboratories, Inc.).

Results

NPe6-PDT alone, but not pemetrexed alone, exerts a strong antitumor effect against human malignant mesothelioma cell lines. We examined the antitumor effects of pemetrexed on MSTO-211H, NCI-H2052, NCI-H2452, and NCI-H28 using the WST assay (Fig. 1A). The IC_{50} values of pemetrexed were 1.2 μM for MSTO-211H, 0.1 μM for NCI-H2052, 10 μM for NCI-H2452, and 8.4 μM for NCI-H28; these values were similar to those in a previous report (25). In MCF-7c3, the IC_{50} value was 5.5 μM (Fig. 1A). Unfortunately, treatment using pemetrexed alone was not sufficient to reach an LD_{90} in the NCI-H2452, and NCI-H28 cell lines, as previously reported (25). On the other hand, NPe6-PDT caused complete cell death in all four cell lines, and NPe6-PDT exerted a strong antitumor effect against MPM *in vitro*, with an LD_{90} being reached in all the cell lines (Fig. 1B). The IC_{50} values were 10 μg/ml of NPe6 and 10 J/cm^2, 33 mW/cm^2 of laser irradiation.

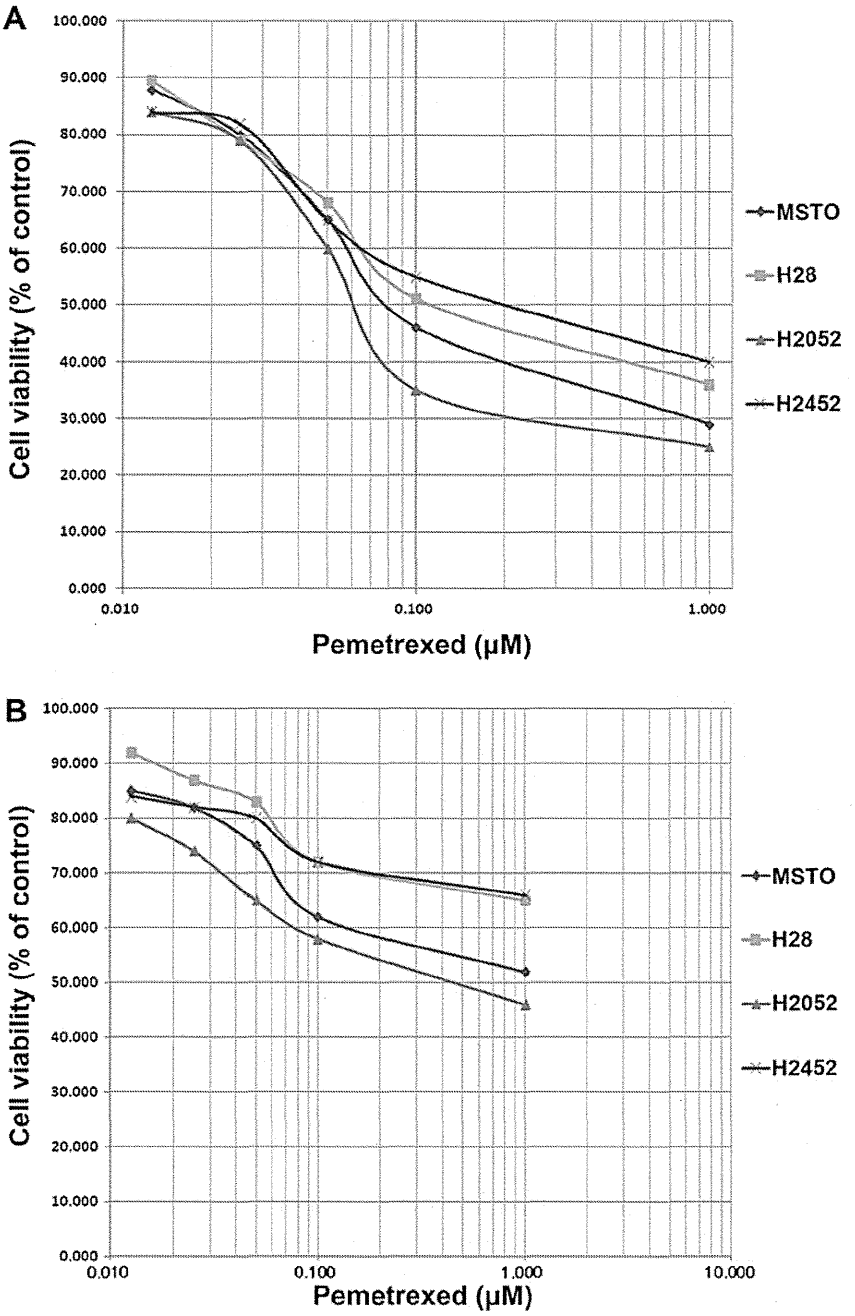

Figure 2. (A) Growth-inhibitory effect of pemetrexed followed by NPe6-PDT in MSTO-211H (♦), H28 (■), H2052 (▲), and H2452 (×) cells. Cells were incubated with 1.2 μM of pemetrexed, which is the IC_{50} dose for MSTO-211H cells; 24 h later, 10 μg/ml of NPe6 was added. Forty-eight hours after the start of treatment, the cells were irradiated with a diode laser (33 mW/cm^2, 10 J/cm^2). These conditions for NPe6-PDT correspond to the IC_{50} dose for MSTO-211H cells. At 72 h after the start of treatment, the growth-inhibitory effect was measured using the WST assay. (B) Growth-inhibitory effect of NPe6-PDT followed by pemetrexed in MSTO-211H (♦), H28 (■), H2052 (▲), and H2452 (×) cells. Cells were incubated with NPe6 (10 μg/ml) for 24 h and then irradiated with a diode laser (33 mW/cm^2, 10 J/cm^2). These conditions for NPe6-PDT correspond to the IC_{50} dose for MSTO-211H cells. The cells were then washed with phosphate buffered saline (PBS), and the medium was replaced with a medium containing pemetrexed; the cells were then cultured for 48 h. At 72 h after the start of treatment, the growth-inhibitory effect was measured using the WST assay.

Pemetrexed enhances the lethal effects of NPe6-PDT against MPM cell lines. We examined the effects of combination therapy using pemetrexed and NPe6-PDT. First, we evaluated whether pemetrexed pre-treatment enhanced the antitumor effect of NPe6-PDT in MPM cells. MPM cells were treated with pemetrexed for 48 h and then were washed with PBS three times; the cells were then incubated for 4 h with NPe6 (10 μg/ml). After incubation, the cells were irradiated with a diode laser (664 nm, 10 J/cm^2), which provided the IC_{50} dose of NPe6-PDT in MSTO-2511 cells. As shown in Fig. 2A, the IC_{50} values were 0.08 μM for the MSTO-211H cells, 0.14 μM for the H28 cells, 0.23 μM for the H2452 cells, and 0.06 μM for the H2052 cells. Thus, pemetrexed treatment followed by NPe6-PDT caused an initial decrease in

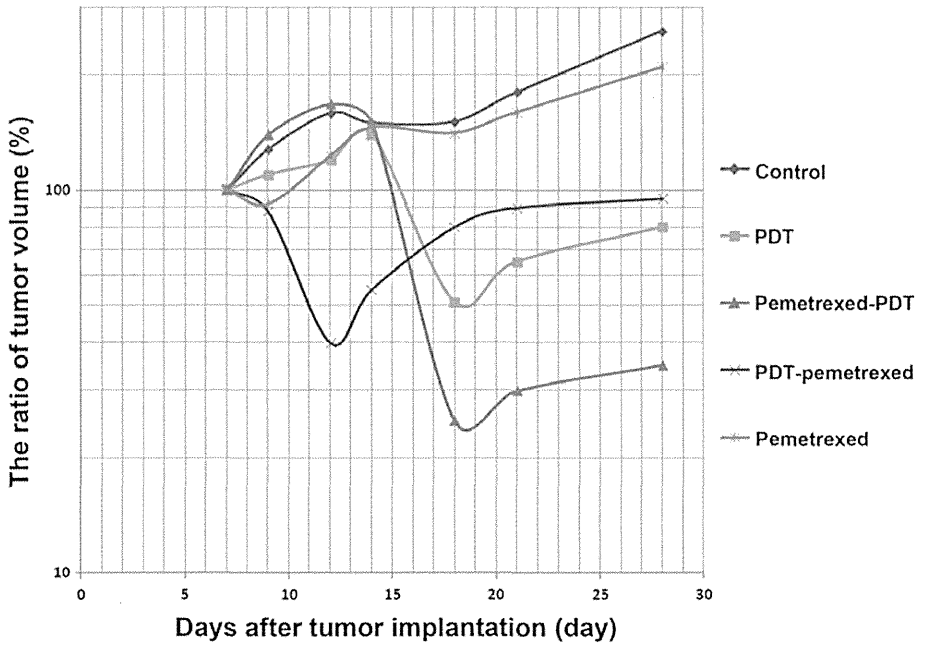

Figure 3. Nude mice transplanted with MSTO-211H tumors measuring 5-7 mm in diameter were treated by pemetrexed and/or NPe6-PDT. The tumor volumes were calculated using the following formula: tumor volume = $LD^2/2$ (L, long diameter; D, short diameter). Untreated MSTO-211H tumors as control (◆, N=10), treated by NPe6-PDT alone (■, N=10), treated by pemetrexed followed by photodynamic therapy (PDT) (▲, N=10), treated by PDT followed by pemetrexed (×, N=10), treated by pemetrexed alone (✳, N=10). For the pemetrexed followed by PDT treatment (▲), mice were intraperitoneally injected with pemetrexed (150 mg/kg daily) on days 7-11; on day 12, the mice were intravenously injected with NPe6 (10 mg/kg) and then irradiated with a 664-nm laser (100 J/cm^2) 2 h later. The laser spot size was 14 mm in diameter, and the power output at the fiber tip was 154 mW. The irradiation time was 16 min and 40 sec. For the PDT followed by pemetrexed treatment (×), mice were intravenously injected with NPe6 (10 mg/kg) and then 2 h later irradiated with a 664-nm laser (100 J/cm^2) on day 7; on days 8-12, the mice were intraperitoneally injected with pemetrexed (150 mg/kg daily). Tumor response was monitored until day 28, and the ratio of the tumor volume was calculated by comparing the volume with tumor volume on day 7.

viability, indicating that pemetrexed enhances the lethal effect of NPe6 (Fig. 2A).

NPe6-PDT followed by pemetrexed treatment yielded no enhancement. We next examined whether NPe6-PDT followed by pemetrexed treatment enhanced the antitumor effect. First, MPM cells were treated with NPe6-PDT using the IC_{50} conditions (NPe6, 10 μg/ml; laser irradiation, 10 J/cm^2). Then, the cells were treated with pemetrexed for 48 h. The survival curves indicated that NPe6-PDT followed by pemetrexed treatment was incapable of obtaining an IC_{50} response except in the H2052 cells, and no enhancement of the treatment effects was observed (Fig. 2B).

Pemetrexed treatment enhanced the antitumor effect of NPe6-PDT against MPM tumors in vivo. We examined the efficacy of combination therapy with NPe6-PDT and chemotherapy using pemetrexed for MPM tumors. We transplanted MSTO-211H cells into nude mice as described in previous reports (33), and then treated the mice with pemetrexed for 5 days. On the sixth day of treatment, we treated the tumors with NPe6-PDT using 10 mg/kg of NPe6 and 10 J/cm^2 of laser irradiation. Fig. 3 shows that pemetrexed pre-treatment followed by NPe6-PDT enabled an 80% loss in the tumor volume and inhibited the re-growth of the tumors. Using this dosage, NPe6-PDT alone decreased the tumor volume by 50%; however, the tumor volume increased once again, reaching the pre-treatment value 10 days after PDT (Fig. 3).

We also evaluated the efficacy of NPe6-PDT followed by pemetrexed treatment, but this treatment schedule did not inhibit the re-growth of the tumor (Fig. 3). NPe6-PDT followed by pemetrexed treatment yielded no enhancement in tumor cell lethality in the *in vivo* experiments, similar to the results *in vitro* (Fig. 3).

Pemetrexed did not stimulate the accumulation of intracellular NPe6 in MSTO-211 cells. To examine the mechanism responsible for the enhancement in cell lethality enabled by pemetrexed pre-treatment followed by NPe6-PDT, we investigated whether pemetrexed stimulates the intracellular accumulation of NPe6 in MSTO-211 cells. MSTO-211 cells were pre-treated for 48 h with an IC_{50} dose of 1.2 μM, then exposed to NPe6 for 3 h. The resulting accumulation of NPe6 was assessed by detecting red fluorescence using fluorescent microscopy (29). No significant difference in the intracellular accumulation of NPe6 was observed between a group with pemetrexed pre-treatment and one without the pre-treatment. Thus, pemetrexed pre-treatment did not enhance the accumulation of intracellular NPe6.

NPe6-PDT induced the expression of TS. The inhibition of TS, resulting in a decrease in thymidine available for DNA synthesis, is reportedly the primary mechanism of pemetrexed (34,35). Therefore, we hypothesized that TS expression may affect the efficacy of combination therapy with pemetrexed and NPe6-PDT. We examined TS protein expression in the MPM cell lines using

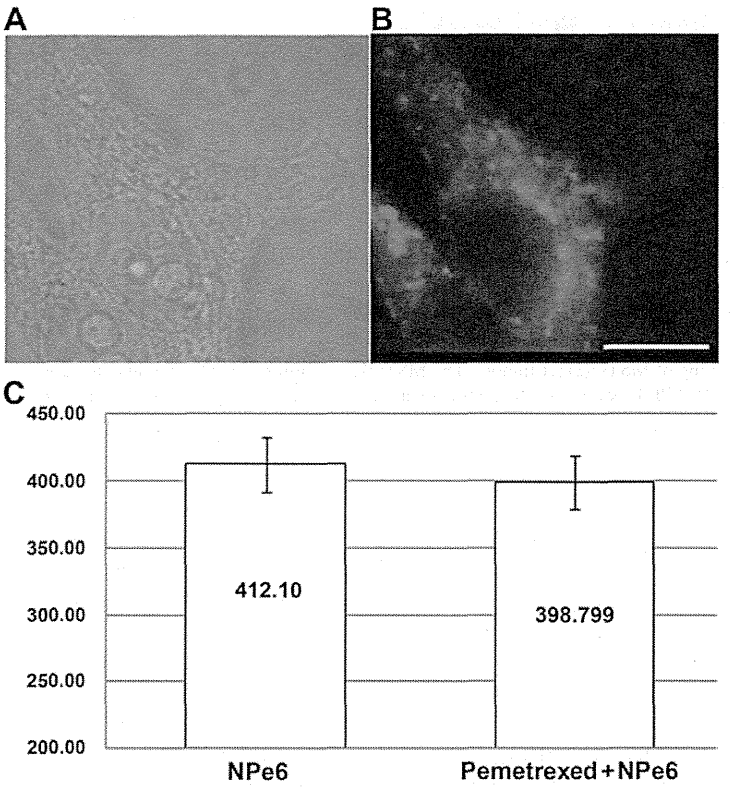

Figure 4. Localization of NPe6 in MSTO-211H cells and fluorescent intensity. Cells were exposed to pemetrexed at the IC_{50} dose of 1.2 μM for 48 h and then were exposed to NPe6 (15 μg/ml) for 4 h; the cells were then washed with phosphate buffered saline (PBS). (A) Image of the cells using white light. (B) The NPe6 in the cells was excited at 405 nm, and red fluorescence was detected using a charged coupled device (CCD) camera system. Scale bar, 5 μm. (C) Fluorescence intensity of NPe6 in cells with or without pemetrexed pre-treatment. The fluorescence intensity of 10 cells was counted, and the average intensity per cell is shown. No and those without pemetrexed pre-treatment.

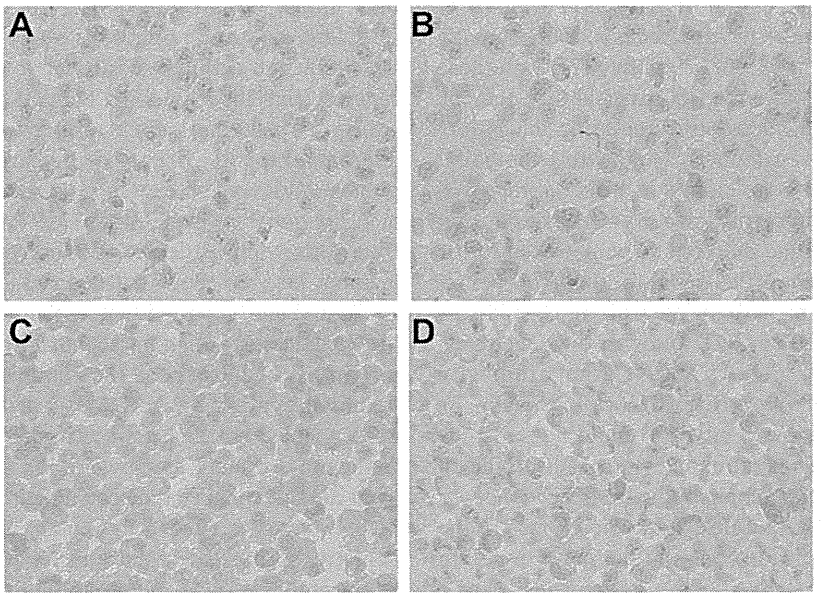

Figure 5. Immunohistochemical staining of human malignant pleural mesothelioma (MPM) cell lines. Immunohistochemical staining using anti-TS antibody (clone 8F1) in (A) MSTO-211H, (B) H2052, (C) H2452, and (D) H29 cells.

an immunohistochemical analysis (Fig. 5). The expression of TS was relatively low in MSTO-211H and NCI-H2052 cells but was relatively high in NCI-H2452 and NCI-H28 cells (Fig. 4). In the *in vivo* model, NPe6-PDT induced TS expression in the MSTO-211H tumors 24 h after the laser irradiation (Fig. 5). These results suggest that the overexpression of TS protein

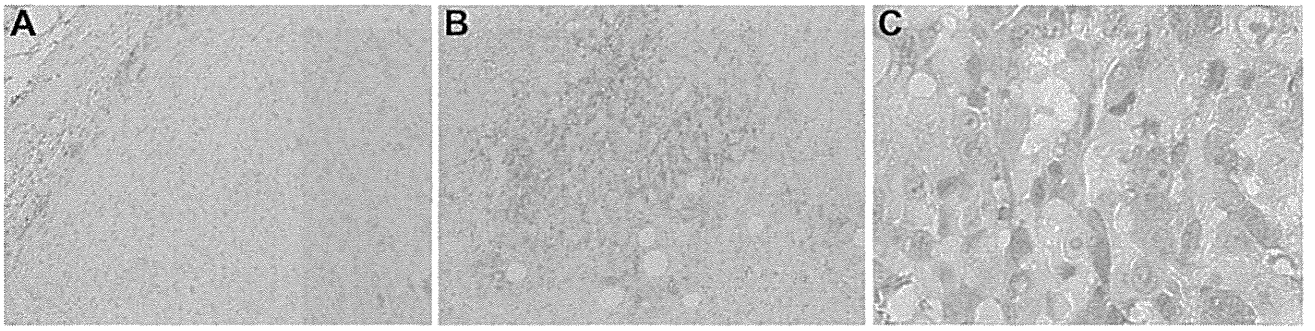

Figure 6. Immunohistochemical staining of MSTO-211H tumors. The MSTO-211H tumors in BALB/c nude mice were collected (A) before photodynamic therapy (PDT) and (B and C) 24 h after PDT. Immunohistochemical staining was performed using anti-TS antibody [magnification in (A) x10; (B) x10; (C) x40].

induced by NPe6-PDT may be associated with the failure of pemetrexed to exert a tumoricidal action. Therefore, we concluded that NPe6-PDT followed by pemetrexed treatment did not enhance tumor cell lethality in the *in vivo* model.

Discussion

Recently, Debefve *et al* reported that PDT affects vascular barrier function and thus increases vessel permeability; this phenomenon may be exploited to facilitate targeted drug delivery (36). Snyder *et al* also reported that a direct vascular effect of PDT at relatively low light doses may be exploited to increase the uptake of systemically circulating drugs to tumors, and this new treatment concept has been named 'photodynamic drug delivery' (37). They developed a novel PDT treatment that enhances the delivery and efficacy of macromolecule-based cancer therapy, such as a liposomally encapsulated formulation of doxorubicin (37). Low-dose PDT reportedly increases microvessel permeability, thereby promoting the controlled release of circulating drugs into tissues; PDT additionally stimulates leukocyte-endothelial cell interactions, mediating the effects of PDT on improved drug delivery (38). Therefore, we hypothesized that NPe6-PDT may enhance the delivery of pemetrexed to the tumors and suspected that NPe6-PDT followed by pemetrexed treatment could provide a synergistic or additive effect *in vivo*. However, NPe6-PDT followed by pemetrexed did not enhance tumor cell lethality, compared with NPe6-PDT alone, either *in vitro* (Fig. 2B) or *in vivo* (Fig. 3). These results indicated that NPe6-PDT could not enhance the antitumor activity of pemetrexed and in fact produced some resistance to treatment, compared with PDT alone.

Pemetrexed reportedly inhibits multiple enzymes in the folate metabolic pathway, with TS being the main target. In NSCLC cell lines, high baseline TS expression levels confer resistance to pemetrexed, and the TS level is correlated with pemetrexed efficacy in a variety of solid tumors. As shown in Fig. 5, the expression of TS was relatively low in MSTO-211 and H2052 cells, which were somewhat more sensitive to pemetrexed than the H2452 and H28 cells (as shown in Fig. 1A). Based on our data shown in Fig. 1A regarding the growth inhibitory effects of pemetrexed, the H2052 cells were the most sensitive to pemetrexed of all the cell lines examined, as in a previous report, because the TS level was relatively low in the H2052 cells, compared with in the H2454 and H28 cells (25). As shown in Fig. 6, NPe6-PDT at the IC_{50} dose induced the expression of TS in MSTO-211 cells. Therefore, based on these results, we concluded that NPe6-PDT followed by pemetrexed treatment did not enhance tumor cell lethality possibly because of the NPe6-PDT-induced expression of TS. Moreover, we previously reported that NPe6-PDT can damage the microvasculature around tumors and induce a vascular shut-down effect, decreasing blood flow to the tumors (17). Sitnik *et al* also reported that PDT-induced microvasculature damage is associated with a significant decrease in the blood flow and severe hypoxia in the tumor (39). We suggested that NPe6-PDT does not enhance the delivery of pemetrexed but may, in fact, obstruct the delivery of pemetrexed to tumors.

Oleinick *et al* reported that photosensitizer accumulation can influence cellular sensitivity to PDT (40). Robey *et al* reported that the expression of ATP-binding cassette (ABC) transport proteins, which render tumor cells resistant to chemotherapeutic drugs, decreases the accumulation of photosensitizers and causes resistance to PDT (41). We have also previously reported that BCRP, a member of the ABC transporter family, decreases the accumulation of Photofrin and may be a molecular determinant (29).

Anand *et al* reported that methotrexate (MTX) stimulated the accumulation of an intracellular photosensitizer, protoporphyrin IX, and enhanced the antitumor effect of PDT using 5-aminolaevulinic acid (ALA), but that ALA-PDT followed by MTX yielded no enhancement in tumor cell lethality (42,43). In the present study, as shown in Fig. 4, pemetrexed pre-treatment did not enhance the accumulation of intracellular NPe6. Further study is needed to explain why the combination of pemetrexed pre-treatment and NPe6-PDT has an additive effect on NPe6-PDT cytotoxicity both *in vitro* and *in vivo*. In conclusion, combination therapy using pemetrexed followed by NPe6 can enhance the cytotoxic effect of NPe6 and has important clinical implications.

Pass *et al* reported that intraoperative PDT did not prolong the survival of patients with MPM (22). However, we recently reported that NPe6-PDT exerted a strong antitumor effect against cancer lesions (29). Therefore, combination treatment using pemetrexed followed by NPe6-PDT may become a new

treatment modality, and further combination with surgery may reduce local recurrence and prolong the survival of patients with malignant mesothelioma.

Acknowledgements

This study was supported in part by a Grant-in-Aid for Scientific Research (C) from Japan Society for the Promotion of Science (JSPS) (to J.U.) (KAKENHI 21591826).

References

1. Peto J, Decarli A, La Vecchia C, Levi F and Negri E: The European mesothelioma epidemic. Br J Cancer 79: 666-672, 1999.
2. Price B: Analysis of current trends in United States mesothelioma incidence. Am J Epidemiol 145: 211-218, 1997.
3. Hodgson JT, McElvenny DM, Darnton AJ, Price MJ and Peto J: The expected burden of mesothelioma mortality in Great Britan from 2002 to 2050. Br J Cancer 92: 587-593, 2005.
4. McCormack V, Peto J, Byrnes G, Straif K and Boffetta P: Estimating the asbestos-related lung cancer burden from mesothelioma mortality. Br J Cancer 106: 575-584, 2012.
5. Van Ruth S, Bass P and Zoetmulder FA: Surgical treatment of malignant pleural mesothelioma: a review. Chest 123: 551-561, 2003.
6. Treasure T, Lang-Lazdunski L, Waller D, Bliss JM, Tan C, Entwisle J, Snee M, O'Brien M, Thomas G, Senan S, O'Byrne K, Kilburn LS, Spicer J, Landau D, Edwards J, Coombes G, Darlison L, Peto J and for the MARS trialists: Extra-pleural pneumonectomy versus no extra-pleural pneumonectomy for patients with malignant pleural mesothelioma: clinical outcomes of the mesothelioma and radical surgery (MARS) randomized feasibility study. Lancet Oncol 12: 763-772, 2011.
7. Pass HI, Kranda K, Temeck BK, Feuerstein I and Steinberg SM: Surgically debulked malignant pleural mesothelioma: results and prognostic factors. Ann Surg Oncol 4: 215-222, 1997.
8. Krug LM, Pass HI, Rusch VW, Kindler HL, Sugarbaker DJ, Rosenzweig KE, Flores R, Friedberg JS, Pisters K, Monberg M, Obasaju CK and Vogelzang NJ: Multicenter phase II trial of neoadjuvant pemetrexed plus cisplatin followed by extrapleural pneumonectomy and radiation for malignant pleural mesothelioma. J Clin Oncol 27: 3007-3013, 2009.
9. Adjei AA: Pemetrexed (ALIMTA), a novel multitargeted antineoplastic agent. Clin Cancer Res 10: 4276s-4280s, 2004.
10. Vogelzang NJ, Porta C and Mutti L: New agents in the management of advanced mesothelioma. Semin Oncol 32: 336-350, 2005.
11. Vogelzang NJ, Rusthoven JJ, Symanowski J, Denham C, Kaukel E, Ruffie P, Gatzemeier U, Boyer M, Emri S, Maneqold C, Niyikiza C and Paoletti P: Phase III study of pemetrexed in combination with cisplatin versus cisplatin alone in patients with malignant pleural mesothelioma. J Clin Oncol 21: 2636-2644, 2003.
12. Rea F, Marulli G, Bortolotti L, Breda C, Favaretto AG, Loreggian L and Sartori F: Induction chemotherapy, extrapleural pneumonectomy (EPP) and adjuvant hemi-thoracic radiation in malignant pleural mesothelioma (MPM): Feasibility and results. Lung Cancer 57: 89-95, 2007.
13. Flores RM, Pass HI, Seshan VE, Dycoco J, Zakowski M, Carbone M, Bains MS and Rusch VW: Extrapleural pneumonectomy versus pleurectomy/decortication in the surgical management of malignant mesothelioma: results in 663 patients. J Thorac Cardiovasc Surg 135: 620-626, 2008.
14. Dougherty TJ, Gomer CJ, Henderson BW, *et al*: Photodynamic therapy. J Natl Cancer Inst 90: 889-905, 1998.
15. Dougherty TJ: An update on photodynamic therapy applications. J Clin Laser Med Surg 20: 3-7, 2002.
16. Edell ES and Cortese DA: Photodynamic therapy in the management of early superficial squamous cell carcinoma as an alternative to surgical resection. Chest 102: 1319-1322, 1992.
17. Kato H, Usuda J, Okunaka T, Furukawa K, Honda H, Sakaniwa N, Suga Y, Hirata T, Ohtani K, Inoue T, Maehara S, Kubota M, Yamada K and Tsuitsui H: Basic and clinical research on photodynamic therapy at Tokyo Medical University Hospital. Lasers Surg Med 38: 371-375, 2006.
18. Kennedy TC, McWilliams A, Edell E, Sutedja T, Downie G, Yung R, Gazdar A, Mahur PN; American College of Chest Physicians: Bronchial intraepithelial neoplasia/early central airways lung cancer: ACCP evidence-based clinical practice guidelines (2nd edition). Chest 132 (Suppl 3): S221-S233, 2007.
19. Krueger T, Altermatt HJ, Mettler D, Scholl B, Magnusson L and Ris HB: Experimental photodynamic therapy for malignant pleural mesothelioma with pegylated mTHPC. Laser Surg Med 32: 61-68, 2003.
20. Friedberg JS, Mick R, Stevenson J, Metz J, Zhu T, Buyske J, Sterman DH, Pass HI, Glatstein E and Hahn SM: A phase I study of Foscan-mediated photodynamic therapy and surgery in patients with mesothelioma. Ann Thorac Surg 75: 952-959, 2003.
21. Ris HB: Photodynamic therapy as an adjunct to surgery for malignant pleural mesothelioma. Lung Cancer 49 (Suppl 1): S65-S68, 2005.
22. Pass HI, Temeck BK, Kranda K, Thomas G, Russo A, Smith P, Friauf W and Steinberg SM: Phase III randomized trial of surgery with or without intraoperative photodynamic therapy and postoperative immunochemotherapy for malignant pleural mesothelioma. Ann Surg Oncol 4: 628-633, 1997.
23. Usuda J, Ichinose S, Ishizumi T, Hayashi H, Ohtani K, Maehara S, Ono S, Honda H, Kajiwara N, Uchida O, Tsutsui H, Ohira T, Kato H and Ikeda N: Outcome of photodynamic therapy using NPe6 for bronchogenic carcinomas in central airways >1.0 cm in diameter. Clin Cancer Res 16: 2198-2204, 2010.
24. Ozasa H, Oguri T, Uemura T, Miyazaki M, Maeno K, Sato S and Ueda R: Significance of thymidylate synthase for resistance to pemetrexed in lung cancer. Cancer Sci 101: 161-166, 2010.
25. O'Kane SL, Eagle GL, Greenman J, Lind MJ and Gawkwell L: COX-2 specific inhibitors enhance the cytotoxic effects of pemetrexed in mesothelioma cell lines. Lung Cancer 67: 160-165, 2010.
26. Usuda J, Chiu SM, Murphy ES, Lam M, Nieminen AL and Oleinick NL: Domain-dependent photodamage to Bcl-2. A membrane anchorage region is needed to form the target of phthalocyanine photosensitization. J Biol Chem 278: 2021-2029, 2003.
27. Usuda J, Hirata T, Ichinose S, Ishizumi T, Inoue T, Ohtani K, Maehara S, Yamada M, Tsutsui H, Okunaka T, Kato H and Ikeda N: Tailor-made approach to photodynamic therapy in the treatment of cancer based on Bcl-2 photodamage. Int J Oncol 33: 689-696, 2008.
28. Kato H, Furukawa K, Sato M, Okunaka T, Kusunoki Y, Kawahara M, *et al*: Phase II clinical study of photodynamic therapy using mono-L-aspartyl chlorine e6 and diode laser for early superficial squamous cell carcinoma of the lung. Lung Cancer 42: 103-111, 2003.
29. Usuda J, Tsunoda Y, Ichinose S, Ishizumi T, Ohtani K, Maehara S, Ono S, Tsutsui H,Ohira T, Okunaka T, Furukawa K, Sugimoto Y, Kato H and Ikeda N: Breast cancer resistant protein (BCRP) is a molecular determinant of the outcome of photodynamic therapy (PDT) for centrally located early lung cancer. Lung Cancer 67: 198-204, 2010.
30. Xue LY, Chiu SM and Oleinick NL: Photodynamic therapy-induced death of MCF-7 human breast cancer cells: a role for caspase-3 in the late steps of apoptosis but not for the critical lethal event. Exp Cell Res 263: 145-155, 2001.
31. Workman P, Aboagye EO, Balkwill F, Balmain A, Bruder G, Chaplin DJ, Double JA, Everitt J, Farningham DA, Glennie MJ, Kelland LR, Robinson V, Stratford IJ, Tozer GM, Watson S, Wedge SR, Eccles SA; Committee of the National Cancer Research Institute: Guidelines for the welfare and use of animals in cancer research. Br J Cancer 102: 1555-1577, 2010.
32. Ohtani K, Usuda J, Ichinose S, Ishizumi T, Hirata T, *et al*: High expression of GADD-45α and VEGF induced tumor recurrence via upregulation of IL-2 after photodynamic therapy using NPe6. Int J Oncol 32: 397-403, 2008.
33. Van TT, Hanibuchi M, Kakiuchi S, Sato S, Kuramoto T, Goto H, Mitsuhashi A, Nishioka Y, Akiyama S and Sone S: The therapeutic efficacy of S-1 against orthotopically implanted human pleural mesothelioma cells in severe combined immunodeficient mice. Cancer Chemother Pharmacol 68: 497-504, 2011.
34. Cappia S, Righi L, Mirabelli D, Ceppi P, Bacillo E, Ardissone F, Molinaro L, Scagliotti GV and Papotti M: Prognostic role of osteopontin expression in malignant pleural mesothelioma. Am J Clin Pathol 130: 58-64, 2008.

35. Righi L, Papotti MG, Ceppi P, Bille A, Bacillo E, Molinaro L, Ruffini E, Scagliotti GV and Selvaggi G: Thymidylate synthase but not excision repair cross-complementation group 1 tumor expression predicts outcome in patients with malignant pleural mesothelioma treated with pemetrexed-based chemotherapy. J Clin Oncol 28: 1534-1539, 2010.
36. Debefve E, Mithieux F, Perentes JY, Wang Y, Cheng C, Schaefer SC, Ruffieux C, Ballini JP, Gonzalez M, van den Bergh H, Ris HB, Lehr HA and Krueger T: Leukocyte-endothelial cell interaction is necessary for photodynamic therapy induced vascular permeabilization. Lasers Surg Med 43: 696-704, 2011.
37. Snyder JW, Greco WR, Bellnier DA, Vaughan L and Henderson BW: Photodynamic therapy: a means to enhanced drug delivery to tumors. Cancer Res 63: 8126-8131, 2003.
38. Wang Y, Perentes JY, Schäfer SC, Gonzalez M, Debefve E, Lehr HA, van den Bergh H and Krueger T: Photodynamic drug delivery enhancement in tumors does not depend on leukocyte-endothelial interaction in a human mesothelioma xenograft model. Eur J Cardiothorac Surg 42: 348-354, 2012.
39. Sitnik TM, Hampton JA and Henderson BW: Reduction of tumor oxygenation during and after photodynamic therapy in vivo: effects of fluence rate. Br J Cancer 77: 1386-1394, 1998.
40. Oleinick NL, Morris RL and Belichenko I: The role of apoptosis in response to photodynamic therapy: what, where, why, and how. Photochem photobiol Sci 1: 1-21, 2002.
41. Robey RW, Steadman K, Polgar O and Bates SE: ABCG2-mediated transport of photosensitizers: potential impact on photodynamic therapy. Cancer Biol Ther 4: 187-194, 2005.
42. Anand S, Honari G, Hasan T, Elson P and Maytin EV: Low-dose methotrexate enhances aminolevulinate-based photodynamic therapy in skin carcinoma cells in vitro and in vivo. Clin Cancer Res 15: 3333-3343, 2009.
43. Sinha AK, Anand S, Ortel BJ, Chang Y, Mai Z, Hasan T and Maytin EV: Methotrexate used in combination with aminolaevulinic acid for photodynamic killing of prostate cancer cells. Br J Cancer 95: 485-495, 2006.

Visceral Pleural Invasion Is Not a Significant Prognostic Factor in Patients With a Part-Solid Lung Cancer

Aritoshi Hattori, MD, Kenji Suzuki, MD, Takeshi Matsunaga, MD, Kazuya Takamochi, MD, and Shiaki Oh, MD

Department of General Thoracic Surgery, Juntendo University School of Medicine, Tokyo, Japan

Background. Visceral pleural invasion (VPI) has been considered to be a prognostic factor. If a tumor shows VPI, it increases the T descriptor and upstages a tumor from stage IA to stage IB pathologically, even for those less than 30 mm in diameter. However, there is still some controversy regarding the prognostic significance of VPI in patients with radiologically early lung cancer with ground glass opacity.

Methods. Between 2004 and 2012, 466 patients with surgically resected pathologic N0 non-small cell lung cancer less than 30 mm in diameter who showed a "part-solid" or "pure-solid" appearance on thin-section computed tomography scan were retrospectively reviewed. A Cox proportional hazard model was used to evaluate prognostic factors. Survival was calculated by the Kaplan-Meier method.

Results. Two hundred thirty-seven patients (55%) showed part-solid and 209 (45%) showed pure-solid nodules on thin-section computed tomography scan. VPI was found in 24 (10%) part-solid nodules and 79 (38%) pure-solid nodules. On the basis of a multivariate analysis, VPI was not a significant prognostic factor in patients with part-solid nodules ($p = 0.5902$). In this group, the 5-year survival rates in patients with and without VPI were 85.6% and 94.9%, respectively ($p = 0.3798$). By contrast, VPI, vessel invasion, maximum tumor diameter, and carcinoembryonic antigen level were significant prognostic factors in patients with pure-solid nodules ($p = 0.0211$, 0.0188, 0.0372, and 0.0492, respectively). Moreover, the 5-year survival in patients with VPI (70.1%) was significantly worse than that in patients without VPI (81.3%) among patients with pure-solid nodules ($p = 0.0051$).

Conclusions. VPI may not contribute to the prognosis of patients with part-solid nodules. Thus, upgrading of the TNM stage on the basis of VPI should be carefully considered in these patients.

(Ann Thorac Surg 2014;98:433–8)

Recent developments in imaging technology and the widespread use of thin-section computed tomography (CT) for screening have made it possible to detect small lung cancers [1]. Radiologically, lung cancers that show a wide area of ground-grass opacity (GGO) are considered to have a favorable prognosis, and in most cases their pathologic features are minimally invasive [2–6]. This cohort has an excellent prognosis, with a recent 5-year survival rate of greater than 90% [6, 7]. On the other hand, radiologically pure-solid lung cancers show more malignant behavior and have a dismal prognosis, with postoperative nodal involvement in approximately 20% of cases, even in clinical stage IA disease [3, 8].

Visceral pleural invasion (VPI) has been considered to be a strong predictor of an adverse prognosis in non-small cell lung cancers (NSCLC), and it increases the T staging factor from T1 to T2 and upstages a tumor from stage IA to stage IB pathologically, even for those less than 30 mm in diameter, based on the TNM staging system for lung cancer [9–11]. This is important because adjuvant chemotherapy is sometimes used in patients with completely resected pathologic stage IB NSCLC but has not been shown to be of value in pathologic stage IA NSCLC [12, 13].

However, there is still some controversy regarding the impact of VPI in patients with lung cancer with GGO lesions on thin-section CT scan because of their minimally invasive nature. Although there is still some controversy regarding the effect of tumor size on the impact of VPI [11, 14, 15], very few series have specifically addressed the prognostic importance of VPI in patients with radiologically small mixed tumors with GGO components (Fig 1). Furthermore, VPI is considered to be strongly related to nodal metastasis. Thus, to evaluate the influence on survival between VPI and small lung cancers based on the findings of thin-section CT scan, we decided to exclude patients with lymph node metastasis. Hence, the aim of this study was to assess the prognostic impact

Accepted for publication April 15, 2014.

Presented at the Poster Session of the Fiftieth Annual Meeting of The Society of Thoracic Surgeons, Orlando, FL, Jan 25–29, 2014.

Address correspondence to Dr Suzuki, Department of General Thoracic Surgery, Juntendo University School of Medicine, 1-3, Hongo 3-chome, Bunkyo-ku, Tokyo, 113-8431, Japan; e-mail: kjsuzuki@juntendo.ac.jp.

Published by Elsevier Inc

0003-4975/$36.00
http://dx.doi.org/10.1016/j.athoracsur.2014.04.084

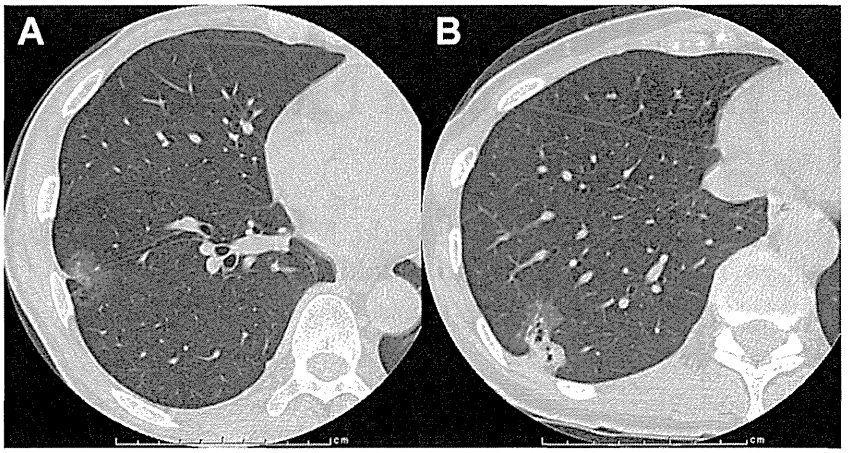

Fig 1. Typical images of part-solid lung cancer on thin-section CT scan. These lesions were proved to present VPI pathologically.

of VPI on survival in patients with node-negative NSCLC among part-solid or pure-solid nodules based on the findings of thin-section CT scan.

Material and Methods

Patients

Between January 2004 and December 2011, 543 patients with surgically resected pathologic N0 (pN0) NSCLC less than 30 mm in diameter were retrospectively reviewed at our institute. None of the patients received neoadjuvant chemotherapy or radiotherapy.

Radiologic Evaluation

For all patients, the findings of preoperative CT were reviewed by the authors (AH, TM, and KS). A contrast-enhanced CT scan was performed to evaluate the entire lung for preoperative staging. The size of the tumors was determined preoperatively on the basis of the findings of thin-section CT scan. In addition, all tumors were subsequently evaluated to estimate the extent of GGO by thin-section CT scan with 2 mm collimation. The lung was photographed with a window level of −500 to −700 H and a window depth of 1000 to 2000 H as a "lung window." The solid component was defined as an area of increased opacification that completely obscured the underlying vascular markings. GGO was defined as an area of a slight homogeneous increase in density that did not obscure the underlying vascular markings.

According to the radiologic findings on thin-section CT, we defined the ratio of the maximum diameter of consolidation to the maximum tumor diameter as the consolidation/tumor ratio (CTR). Pure GGO was defined as a tumor with CTR equal to 0. A part-solid nodule was defined as a tumor with focal nodular opacity that contained both solid and GGO components ($0 < CTR < 1.0$), and a pure-solid nodule was defined as a tumor that only showed consolidation without GGO ($CTR = 1.0$). In this study, 97 patients with pure GGO were excluded from this study because such tumors are pathologically less invasive [2, 3] and this cohort lacked findings of VPI (ie, VPI was never found in 97 patients with pure GGO in this study), and 466 patients with surgically resected pN0 NSCLC less than 30 mm in diameter who showed a part-solid or pure-solid appearance on thin-section CT scan were retrospectively reviewed.

Pathologic Evaluation

To evaluate of VPI, all sections were stained in our institute by the elastic van Gieson method to assess the presence or absence of preservation of the preexisting elastic layer of the visceral pleura. VPI was classified according to the Japan Lung Cancer Society [16] and International Union Against Cancer TNM [11] criteria: PL0 represents tumor either within the subpleural lung parenchyma or invading superficially into the pleural connective tissue beneath the elastic layer, PL1 represents a tumor that invades beyond the elastic layer but is not exposed on the pleural surface, and PL2 represents a tumor that is exposed on the pleural surface but does not involve adjacent anatomic structures. In this study, pathologic PL0 status was defined as without VPI, whereas pathologic PL1 and PL2 were defined as with VPI.

In addition, vessel invasion (ie, pathologic lymphatic and vascular invasion) was determined by the identification of tumor cells in the lymphatic lumen or vein vessel lumen. To assess lymphatic and vascular invasion, all sections were stained by D2-40 to assess the presence or absence of preservation of vessel invasion in our institute.

Operative Policy

Regarding the operation, major lung resection with systemic lymph node dissection was warranted for a pure-solid tumor in our institute, whereas segmentectomy is now indicated for part-solid or pure-solid lung cancers 2 cm or smaller according to the Japan Clinical Oncology Group [17]. Nonanatomic wedge resection was performed for a few elderly patients or for patients with high cardiopulmonary risk. By contrast, we basically adopt limited resection for very early lung cancer such as pure GGO lesions, which are considered to be less invasive.

With regard to the proper selection of wedge resection or segmentectomy for early lung cancer, operative modes were selected in accordance with the findings of thin-section CT scan (ie, consolidation/tumor ratio) and the tumor location (ie, peripheral or central) to obtain sufficient surgical margins.

Statistics

With institutional review board approval, the medical record of each patient was reviewed with regard to gender, age, pack/year smoking, pathological T status, VPI, vessel invasion, maximum tumor dimension on thin-section CT scan, serum carcinoembryonic antigen level (CEA) (ng/mL) and CTR. The associations of VPI with several clinicopathologic variables were assessed by Fisher's exact test or the χ^2 test. Cumulative survival rates in each group (ie, part-solid nodule or pure-solid nodule) were calculated by the Kaplan-Meier estimation method, the date of surgical resection being used as the starting point and the date of death of all causes or the last follow-up date as the endpoint. Univariate and multivariate analyses were used to identify the clinical factors that significantly predicted the prognosis in patients with surgically resected pN0 part-solid or pure-solid lung cancer less than 30 mm in diameter. A univariate analysis was performed by the log-rank test. A multivariate analysis was performed by the Cox proportional hazard model using SPSS Statistics 21 (SPSS Inc.). Forward and backward stepwise procedures were used to determine the combination of factors that were essential for predicting the prognosis. Continuous data are shown with means and standard deviation (SD) for normality. The results of a statistical analysis were considered to be significant when the probability value was less than 0.05.

Results

Among 466 eligible patients with surgically resected pN0 NSCLC less than 30 mm in diameter, 209 (45%) showed pure-solid nodules and 237 (55%) showed part-solid nodules on thin-section CT scan. Two hundred twenty-five patients were men and 221 were women. The patients ranged in age from 24 to 89 years, with an average of 66 years. The overall patient characteristics based on the findings of thin-section CT scan are shown in Table 1. VPI was found in 103 (23%) of all eligible patients. Among them, VPI was found in 79 (38%) patients with pure-solid nodules and in 24 (10%) with part-solid nodules ($p < 0.0001$). By contrast, VPI was not found in any of the 97 patients with pure-GGO on thin-section CT scan.

With regard to the relationships between VPI and clinicopathologic factors, VPI was found to be significantly associated with gender, smoking status, pathologic maximum tumor dimension, CEA titer, vessel invasion, histologic type, and CTR in patients with surgically resected pN0 part-solid or pure-solid lung cancer less than 30 mm in diameter (Table 2).

The overall 5-year survival rate for 466 eligible lung cancer patients was 85.5%, and the overall median follow-up period after lung resection was 41.2 months. In this cohort, the 5-year survival rate in 363 patients without VPI (89.6%) was significantly better than that in 103 patients with VPI (73.5%) ($p < 0.0001$).

Among the patients with pure-solid nodules, 128 were men and 81 were women, with an average age of 67 years. The 5-year survival rate of patients with pN0 pure-solid lung cancer less than 30 mm in diameter was 76.9%. On the basis of a multivariate analysis for overall survival, VPI, vessel invasion, maximum tumor diameter, and CEA were significant prognostic factors in patients with pure-solid nodules ($p = 0.0211$, 0.0188, 0.0372, and 0.0492, respectively) (Table 3). Moreover, the 5-year survival rate in patients with VPI (70.1%) was significantly worse than that in patients without VPI (81.3%) ($p = 0.0051$) (Fig 2).

Table 1. Overall Patient Characteristics

Factor	Part-Solid Nodule, n (%)	Pure-Solid Nodule, n (%)
Total (n = 446)	237	209
Age, y		
>70	157 (66.2)	121 (57.9)
≤70	80 (33.8)	88 (32.1)
Gender		
Male	97 (40.9)	128 (61.2)
Female	140 (59.1)	81 (38.8)
Pack/year smoking		
>20	167 (70.5)	96 (45.9)
≤20	70 (29.5)	113 (54.1)
Maximum tumor dimension (pathologic)		
p-T1a	169 (71.3)	134 (64.1)
p-T1b	68 (28.7)	75 (35.9)
Carcinoembryonic antigen (ng/mL)		
≥3	173 (73.0)	107 (51.2)
<3	64 (27.0)	102 (48.8)
Visceral pleural invasion		
Absence	213 (89.9)	130 (62.2)
Presence	24 (10.1)	79 (37.8)
Vessel invasion[a]		
Presence	56 (23.6)	146 (69.9)
Absence	181 (76.4)	63 (30.1)
Histologic type		
Adenocarcinoma	234 (98.7)	167 (79.9)
Squamous cell carcinoma	2 (0.8)	38 (18.2)
Other NSCLC	1 (0.5)	4 (1.9)
Consolidation tumor ratio (CTR)		
0 < CTR ≤ 0.5	103 (43.5)	0
0.5 < CTR < 1.0	134 (56.5)	0
CTR = 1.0	0	209 (100)
Operation		
Limited resection (wedge/segmentectomy)	83 (35.0)	44 (22.0)
Major lung resection (lobectomy)	154 (65.0)	163 (78.0)

[a] Vessel invasion includes pathologic lymphatic and vascular invasion.

NSCLC = non-small cell lung cancer.

Table 2. Relationships Between Status of Pleural Invasion and Several Clinicopathologic Factors in Patients With Pathologic N0 Part-Solid or Pure-Solid Lung Cancer <30 mm in Diameter

Factors	Absence of VPI, n (%)	Presence of VPI, n (%)	*p* Value[a]
Total (n = 446)	n = 343	n = 103	
Gender			
Male	161 (46.9)	64 (62.1)	0.0068
Female	182 (53.1)	39 (37.9)	
Pack/year smoking			
>20	217 (63.3)	47 (45.6)	0.0032
≤20	126 (26.7)	56 (54.4)	
Maximum tumor dimension (pathologic)			
T1a	245 (71.4)	58 (56.3)	0.0039
T1b	98 (28.6)	45 (43.7)	
Carcinoembryonic antigen (ng/mL)			
≥3	228 (66.5)	52 (50.5)	0.0032
<3	115 (33.5)	51 (49.5)	
Vessel invasion[b]			
Absence	244 (71.1)	20 (19.4)	<0.0001
Presence	99 (28.9)	83 (80.6)	
Histologic type			
Adenocarcinoma	311 (90.7)	80 (77.6)	0.0003
Squamous cell carcinoma	7 (2.0)	8 (7.8)	
Other NSCLC	25 (7.3)	15 (14.6)	
Consolidation tumor ratio (CTR)			
0 < CTR < 1.0	213 (62.1)	24 (23.3)	<0.0001
CTR = 1.0	130 (37.9)	79 (76.7)	

[a] *p* value in χ^2 test. [b] Vessel invasion includes pathologic lymphatic and vascular invasion.

NSCLC = non-small cell lung cancer; VPI = visceral pleural invasion.

The group with part-solid nodules included 97 men and 140 women, with an average age of 66 years. The 5-year survival rate of patients with pN0 part-solid lung cancer less than 30 mm in diameter was 93.6%. On the basis of a multivariate analysis for overall survival, CEA and CTR were significant prognostic factors in patients with part-solid nodules ($p = 0.0295$ and 0.0195). By contrast, VPI was not a significant prognostic factor for overall survival according to a multivariate analysis among patients who showed part-solid nodules on thin-section CT scan ($p = 0.5902$) (Table 4). With regard to the relationship between the presence or absence of VPI and CTR in patients with a part-solid nodule, the patients with VPI showed significantly larger CTR than did the patients without VPI (mean CTR, 0.738 vs 0.557; $p < 0.0001$).

Regarding the overall survival rate, we did not find a significant difference between patients without VPI (94.9%) and with VPI (85.6%) in the group with part-solid lung cancer ($p = 0.3798$) (Fig 3). Furthermore, a significant difference was not shown in recurrence-free survival between patients without VPI (93.2%) and with VPI (86.1%) in the group with part-solid lung cancer ($p = 0.6489$).

Comment

Visceral pleural invasion (VPI) has long been recognized as an adverse prognostic factor in NSCLC and has been included in the TNM staging as a pivotal factor that should upstage the pathologic T factor [9–11, 18, 19]. This is important because the distinction between pathologic stage IA and stage IB has been helpful for identifying patients who may benefit from adjuvant chemotherapy. Several recent randomized clinical trials have shown that patients with pathologic stage IB NSCLC significantly benefit from adjuvant chemotherapy, but this has not been shown to be of value in pathologic stage IA disease [12, 13].

By contrast, the ability of VPI to reflect the T factor status remains controversial because elastic stains are not widely used to uniformly define VPI [11, 15, 20]. Furthermore, there has been no suggestion of an association between VPI and the N factor in the TNM system despite the significant correlation between lymph node metastasis and VPI [18, 21]. To address these issues, we

Table 3. Results of Univariate and Multivariate Analyses for Overall Survival in Patients with Pathologic N0 Non-Small Cell Lung Cancer <30 mm in Diameter With a Pure-Solid Appearance on Thin-Section CT Scan

	Univariate			Multivariate		
Variable	HR	95% CI	*p* Value[a]	HR	95% CI	*p* Value[a]
Gender (female)	0.520	0.244–1.107	0.0899	0.556	0.224–1.382	0.2061
Pack/year	1.006	0.998–1.015	0.1286	1.432	0.614–3.340	0.4061
Maximum tumor dimension (mm)	0.426	0.220–0.824	0.0113	0.502	0.253–0.998	0.0492
CEA (ng/mL)	0.365	0.179–0.743	0.0054	0.445	0.208–0.953	0.0372
Visceral pleural invasion (absence)	0.396	0.203–0.775	0.0068	0.445	0.224–0.886	0.0211
Vessel invasion (absence)[b]	0.184	0.056–0.601	0.0051	0.235	0.070–0.787	0.0188
Histology (adenocarcinoma)	0.564	0.285–1.113	0.0985	0.712	0.355–1.396	0.3600
Operation (limited resection)	1.434	0.672–3.060	0.3511	1.338	0.601–2.979	0.4673

[a] *p* value in a Cox proportional hazard model. [b] Vessel invasion includes pathologic lymphatic and vascular invasion.

CEA = carcinoembryonic antigen; CI = confidence interval; HR = hazard ratio.

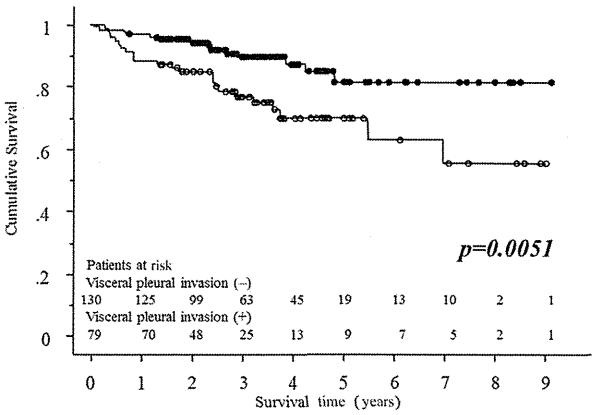

Fig 2. Survival curves for patients with surgically resected pure-solid lung cancers less than 30 mm in diameter based on thin-section computed tomographic findings. A statistically significant difference was observed between the outcomes with and without visceral pleural invasion (5-year overall survival rate, 81.3% vs 70.1%; log-rank test; p = 0.0051).

evaluated all sections by the elastic van Gieson method to precisely assess the presence or absence of the preexisting elastic layer of the visceral pleura. Furthermore, patients with nodal metastasis were excluded from this study to eliminate other confounders of the prognosis and to focus on the relationship between VPI and small lung cancer less than 30 mm in diameter based on the findings of thin-section CT scan (ie, part-solid or pure-solid nodule).

On the basis of our results, VPI has significant value in predicting survival in patients with radiologically pure-solid lung cancer despite their small size. However, VPI may not contribute to the prognosis in patients with part-solid lung cancers. Thus, upgrading of TNM staging and the administration of postoperative chemotherapy on the basis of pleural factors should not be considered in lung cancer patients with GGO predominance.

In fact, radiologic findings of GGO and consolidation have been shown to be well correlated with a pathologically less invasive nature of early-stage NSCLC [6]. On the basis of these results, whereas VPI is a significant prognostic factor regarding survival in patients with pure-solid nodules (ie, invasive lung cancers), CTR is a more reliable prognostic indicator than VPI in patients with small lung cancer with a GGO component. The greatest concern is the mechanism of the disruption of the visceral pleural elastic layer in patients with early-stage NSCLC including GGO lesions.

In the current study, pure-GGO lesions were excluded because VPI was never observed in these patients owing to their minimally invasive nature and the inability to penetrate a thick elastic layer. By contrast, among approximately 10% of the part-solid tumors that showed VPI, a solid component is considered to have strongly contributed to the invasion of the visceral pleural elastic layer in these patients based on both the pathologic and radiologic findings, as indicated in Figure 1. However, the greatest reason for not including VPI as a prognostic factor in patients with part-solid lung cancer may be the difference in malignant behavior between pure-solid and part-solid tumors with a GGO component in small NSCLC [22]. Pure-solid tumors show more malignant potential and have a worse prognosis with a high frequency of postoperative nodal involvement compared with part-solid tumors, even when the solid component is the same size in both types of tumor [23]. Thus, VPI plays a completely different role in each subtype of early-stage NSCLC based on the findings of thin-section CT scan. Therefore, upstaging from T1 to T2 based on the presence of pleural invasion should be carefully considered in patients with early-stage lung cancer with a GGO component.

One of the advantages in this study was the reliability of pathologic assessment because staining of the visceral pleural elastic layer with the elastic van Gieson method was performed for all sections to evaluate VPI more precisely. By contrast, this study was limited by a relatively short median follow-up period, and a number of patients with VPI in part-solid nodules was relatively small. Thus, further investigations are warranted.

In conclusion, among patients with pathologic N0 lung cancer less than 30 mm in diameter, the prognostic

Table 4. Results of Univariate and Multivariate Analyses for Overall Survival in Patients with Pathologic N0 Non-Small Cell Lung Cancer <30 mm in Diameter with a Part-Solid Appearance on Thin-Section CT Scan

	Univariate			Multivariate		
Variable	HR	95% CI	p Value[a]	HR	95% CI	p Value[a]
Gender (female)	0.608	0.176–2.102	0.4318	1.369	0.217–5.546	0.7117
Pack/year	1.016	0.998–1.034	0.0836	1.015	0.991–1.041	0.2160
Maximum tumor dimension (mm)	1.014	0.926–1.111	0.7625	1.007	0.896–1.131	0.9126
CEA (ng/mL)	1.150	1.032–1.283	0.0118	1.152	1.014–1.308	0.0295
Visceral pleural invasion (absence)	0.355	0.075–1.676	0.1907	0.632	0.119–3.352	0.5902
Vessel invasion (absence)[b]	0.323	0.093–1.118	0.0744	0.249	0.048–1.284	0.0966
Consolidation tumor ratio (<0.5)	0.193	0.041–0.912	0.0379	0.135	0.025–0.724	0.0195
Operation (limited resection)	1.207	0.349–4.177	0.7669	3.446	0.719–16.515	0.1217

[a] p value in a Cox proportional hazard model. [b] Vessel invasion includes pathologic lymphatic and vascular invasion.

CEA = carcinoembryonic antigen; CI = confidence interval; HR = hazard ratio.

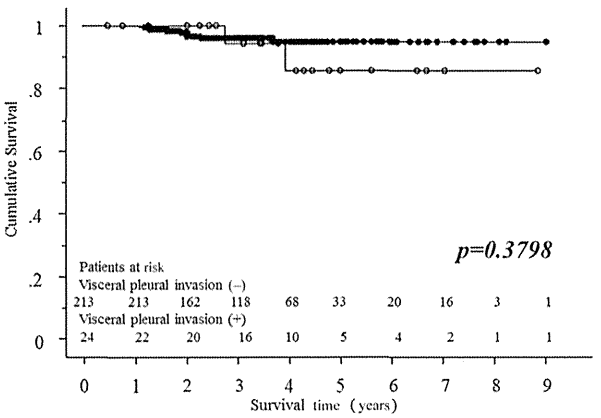

Fig 3. Survival curves for patients with surgically resected part-solid lung cancers less than 30 mm in diameter based on thin-section computed tomographic findings. A statistically significant difference was not observed between the outcomes with and without visceral pleural invasion (5-year overall survival rate, 94.9% vs 85.6%; log-rank test; p = 0.3798).

impact of VPI may be completely different in different subtypes according to the findings on thin-section CT scan. VPI is clearly a significant prognostic factor in patients with pure-solid nodules. For these patients, upstaging of the T factor is mandatory. However, VPI may not contribute to the prognosis in patients with small lung cancer with a part-solid appearance. The proper indications for upstaging of the T factor based on pleural invasion is clinically important because of the impact of pathologic stage IA versus stage IB status on survival and the consequent issue regarding the administration of adjuvant chemotherapy after surgical procedures on the lung. It is hoped that these issues regarding the importance of a GGO component will be addressed in the prospective IASLC lung cancer staging project.

Supported in part by a grant-in-aid for cancer research from the Ministry of Health, Labour and Welfare, Japan, and the Smoking Research Foundation.

References

1. Aberle DR, Adams AM, Berg CD, et al. Reduced lung-cancer mortality with low-dose computed tomographic screening. N Engl J Med 2011;365:395–409.
2. Travis WD, Brambilla E, Noguchi M, et al. International Association for the Study of Lung Cancer/American Thoracic Society/European Respiratory Society international multidisciplinary classification of lung adenocarcinoma. J Thorac Oncol 2011;6:24485.
3. Suzuki K, Kusumoto M, Watanabe S, Tsuchiya R, Asamura H. Radiologic classification of small adenocarcinoma of the lung: radiologic-pathologic correlation and its prognostic impact. Ann Thorac Surg 2006;81:4139.
4. Takamochi K, Nagai K, Yoshida J, et al. The role of computed tomographic scanning in diagnosing mediastinal node involvement in non-small cell lung cancer. J Thorac Cardiovasc Surg 2000;119:113540.
5. Suzuki K, Asamura H, Kusumoto M, Kondo H, Tsuchiya R. "Early" peripheral lung cancer: prognostic significance of ground glass opacity on thin-section computed tomographic scan. Ann Thorac Surg 2002;74:16359.
6. Suzuki K, Koike T, Asakawa T, et al. A prospective radiological study of thin-section computed tomography to predict pathological noninvasiveness in peripheral clinical IA lung cancer (Japan Clinical Oncology Group 0201). J Thorac Oncol 2011;6:7516.
7. Asamura H, Hishida T, Suzuki K, et al. Radiographically determined noninvasive adenocarcinoma of the lung: survival outcomes of Japan Clinical Oncology Group 0201. J Thorac Cardiovasc Surg 2013;146:24–30.
8. Hattori A, Suzuki K, Matsunaga T, et al. Is limited resection appropriate for radiologically "solid" tumors in small lung cancers? Ann Thorac Surg 2012;94:2125.
9. Rami-Porta R, Ball D, Crowley J, et al. The IASLC Lung Cancer Staging Project: proposals for the revision of the T descriptors in the forthcoming (seventh) edition of the TNM classification for lung cancer. J Thorac Oncol 2007;2:593–602.
10. Butnor KJ, Travis WD. Recent advances in our understanding of lung cancer visceral pleural invasion and other forms of minimal invasion: implications for the next TNM classification. Eur J Cardiothorac Surg 2013;43:309–11.
11. Travis WD, Brambilla E, Rami-Porta R, et al. Visceral pleural invasion: pathologic criteria and use of elastic stains: proposal for the 7th edition of the TNM classification for lung cancer. J Thorac Oncol 2008;3:1384–90.
12. Tsuboi M, Ohira T, Saji H, et al. The present status of postoperative adjuvant chemotherapy for completely resected non-small cell lung cancer. Ann Thorac Cardiovasc Surg 2007;13:73–7.
13. Kato H, Ichinose Y, Ohta M, et al. A randomized trial of adjuvant chemotherapy with uracil-tegafur for adenocarcinoma of the lung. N Engl J Med 2004;350:1713–21.
14. David E, Thall PF, Kalhor N, et al. Visceral pleural invasion is not predictive of survival in patients with lung cancer and smaller tumor size. Ann Thorac Surg 2013;95:1872–7; discussion 1877.
15. Butnor KJ, Cooper K. Visceral pleural invasion in lung cancer: recognizing histologic parameters that impact staging and prognosis. Adv Anat Pathol 2005;12:1–6.
16. Japan Lung Cancer Society. Classification of Lung Cancer. Seventh Edition. Tokyo: Kanehara Publishing; 2009.
17. Nakamura K, Saji H, Nakajima R, et al. A phase III randomized trial of lobectomy versus limited resection for small-sized peripheral non-small cell lung cancer (JCOG0802/WJOG4607L). Jpn J Clin Oncol 2011;40:271–4.
18. Yoshida J, Nagai K, Asamura H, et al. Visceral pleura invasion impact on non-small cell lung cancer patient survival: its implications for the forthcoming TNM staging based on a large-scale nation-wide database. J Thorac Oncol 2009;4:959–63.
19. Kawase A, Yoshida J, Miyaoka E, et al. Visceral pleural invasion classification in non-small-cell lung cancer in the 7th edition of the tumor, node, metastasis classification for lung cancer: validation analysis based on a large-scale nationwide database. J Thorac Oncol 2013;8:606–11.
20. Taube JM, Askin FB, Brock MV, Westra W. Impact of elastic staining on the staging of peripheral lung cancers. Am J Surg Pathol 2007;31:953–6.
21. Shimizu K, Yoshida J, Nagai K, et al. Visceral pleural invasion is an invasive and aggressive indicator of non-small cell lung cancer. J Thorac Cardiovasc Surg 2005;130:160–5.
22. Maeyashiki T, Suzuki K, Hattori A, et al. The size of consolidation on thin-section computed tomography is a better predictor of survival than the maximum tumour dimension in resectable lung cancer. Eur J Cardiothorac Surg 2012;43:915–8.
23. Tsutani Y, Miyata Y, Yamanaka T, et al. Solid tumors versus mixed tumors with a ground-glass opacity component in patients with clinical stage IA lung adenocarcinoma: prognostic comparison using high-resolution computed tomography findings. J Thorac Cardiovasc Surg 2012;146:17–23.

Role of lymphatic invasion in the prognosis of patients with clinical node-negative and pathologic node-positive lung adenocarcinoma

Takahiro Mimae, MD, PhD,[a] Yasuhiro Tsutani, MD, PhD,[a] Yoshihiro Miyata, MD, PhD,[a] Tomoharu Yoshiya, MD,[a] Yuta Ibuki, MD,[a] Kei Kushitani, MD, PhD,[b] Yukio Takeshima, MD, PhD,[b] Haruhiko Nakayama, MD, PhD,[c] Sakae Okumura, MD, PhD,[d] Masahiro Yoshimura, MD, PhD,[e] and Morihito Okada, MD, PhD[a]

Objective: Some patients with clinical T1 N0 M0 lung adenocarcinoma have pathologic lymph node metastasis. However, neither the precise prognosis nor the factors predictive of the prognosis of such patients have yet been identified.

Methods: Our study included 609 patients with clinical T1 N0 M0 lung adenocarcinoma; 568 (93.3%) pathologic node negative [pN(–)] and 41 (6.7%) pathologic node positive [pN(+)] patients, diagnosed after complete surgical resection. The association between prognosis and pathologic findings was analyzed retrospectively.

Results: pN(+) patients had a significantly lower lepidic growth component ratio (10% vs 50%), a higher lymphatic invasion (LI) rate (68% vs 11%), vessel invasion rate (59% vs 14%), and visceral pleural invasion rate (29% vs 9%), compared with pN(–) patients (all *P*s < .001). Surprisingly, 13 of 41 (32%) pN(+) patients showed no LI. In pN(–) patients, a multivariate analysis of recurrence-free survival revealed that lower lepidic growth component ratio, and lymphatic, vessel, and pleural invasion were significantly correlated with a poor prognosis ($P = .008$, .045, .031, and .024). However, in pN(+) patients, the multivariate analysis of recurrence-free survival showed that only LI was a significant independent prognostic factor ($P = .037$). The 5-year recurrence-free survival rates were as follows: 91.2% for pN(–)/LI(–) patients, 68.2% for pN(–)/LI(+) patients, 63.5% for pN(+)/LI(–) patients, and 41.9% for pN(+)/LI(+) patients. LI status stratified the prognosis not only in patients with no nodal metastasis but also in those with metastasis.

Conclusions: LI, which is not always present in node-positive adenocarcinoma, is an important prognostic variable in patients with node involvement. (J Thorac Cardiovasc Surg 2014;147:1820-6)

Fluorescence deoxyglucose (FDG) positron emission tomography (PET) is commonly used for preoperative assessment of primary tumors, lymph nodes, and distant metastasis to determine staging and treatment strategy,[1-3] thereby improving the accuracy of the definition of clinical stage IA compared with only computed tomography assessment.[1] This has changed the population of patients with clinical stage IA lung adenocarcinoma.[1,4-7] However, some clinical lymph node-negative [cN(–)] patients show positive pathologic lymph node [pN(+)] metastasis. It is speculated that a cN(–) but pN(+) status indicates an initial lymph node metastatic condition, because the accumulation of FDG in the lymph node could be significantly higher in patients with massive lymph node metastasis. Therefore, cN(–)/pN(+) patients may have a better prognosis than cN(+)/pN(+) patients, or a similar prognosis to cN(–)/pN(–) patients. In addition, no studies have identified the prognostic factors in cN(–)/pN(+) patients.

In our study, we evaluated the clinicopathologic findings and prognosis of patients with clinical T1 N0 M0 lung adenocarcinoma according to lymph node status, or other pathologic status. First, we examined the pathologic findings to identify predictive factors for recurrence-free survival (RFS) among patients with clinical stage IA lung adenocarcinoma. Multivariate analysis revealed that lymphatic invasion (LI) status was a predictive factor, both in patients with and without node involvement. Next, we assessed the prognosis of patients with and without lymph node involvement according to LI status. The results highlight the importance of the LI status in patients with clinical T1 N0 M0 lung adenocarcinoma.

MATERIALS AND METHODS

Patient Population

Our study included 611 patients who underwent complete surgical resection of clinical stage IA lung adenocarcinoma at the Hiroshima University

From the Departments of Surgical Oncology[a] and Pathology,[b] Hiroshima University, Hiroshima, Japan; Department of Thoracic Surgery,[c] Kanagawa Cancer Center, Yokohama, Japan; Department of Thoracic Surgery,[d] Cancer Institute Hospital, Tokyo, Japan; and Department of Thoracic Surgery,[e] Hyogo Cancer Center, Akashi, Japan.

Disclosures: Authors have nothing to disclose with regard to commercial support.
Received for publication Aug 5, 2013; revisions received Oct 22, 2013; accepted for publication Nov 22, 2013; available ahead of print Feb 7, 2014.

Address for reprints: Morihito Okada, MD, PhD, Department of Surgical Oncology, Hiroshima University, Hiroshima, Japan, 1-2-3 Kasumi, Minami-ku, Hiroshima, 734-8551, Japan (E-mail: morihito1217@hiroshima-u.ac.jp).

0022-5223/$36.00

http://dx.doi.org/10.1016/j.jtcvs.2013.11.050

Abbreviations and Acronyms

CT = computed tomography
FDG = fluorescence deoxyglucose
GGO = ground glass opacity
HU = Haunsfield unit
LC = lepidic component
LI = lymphatic invasion
OS = overall survival
PET = positron emission tomography
RFS = recurrence-free survival
SUV = standardized uptake value

Hospital (Hiroshima, Japan), the Kanagawa Cancer Centre (Yokohama, Japan), the Cancer Institute Hospital (Tokyo, Japan), and the Hyogo Cancer Centre (Akashi, Japan) between April 2007 and December 2010. Approval was given by the institutional review boards of the participating institutions, all of which waived the requirement for informed consent from individual patients for this retrospective review of the prospective database. Two patients were excluded because they lacked a lepidic component (LC) ratio. The data from the remaining 609 patients were analyzed retrospectively. High-resolution computed tomography (CT) and FDG-PET/CT, followed by a curative R0 resection were performed for all patients staged according to the TNM Classification of Malignant Tumours.[8] Endobronchial ultrasonography or mediastinoscopy was not performed routinely because all patients underwent preoperative high-resolution CT and FDG-PET/CT; the high-resolution CT results showed no swelling of mediastinal or hilar lymph nodes and FDG-PET revealed no accumulation of FDG in those lymph nodes. Lymph node swelling was defined when the diameter of a minor axis is larger than 10 mm. Sublobar resection was performed in cases of complete removal of the disease with appropriate surgical margins for a peripheral T1a N0 M0 tumor. Wedge resection without lymph node assessment was performed for ground glass opacity (GGO) tumors on high-resolution CT, which was regarded as a node-negative and noninvasive tumor in a prospective study.[9] Segmentectomy with hilar and mediastinal lymph node dissection were performed for a GGO-mixed tumor. If lymph node involvement was detected on an intraoperative frozen section of any lymph node, the procedure was converted to a standard lobectomy. All other patients underwent a standard lobectomy. The inclusion criteria included preoperative staging determined by high-resolution CT and FDG-PET/CT, curative surgery without any induction therapy, and a definitive histopathologic diagnosis of lung adenocarcinoma. Patients with incompletely resected tumors (R1 or R2), and those with multiple tumors or previous lung surgery, were excluded from the data set.

Pathology Studies

Sections were fixed with 10% formalin and embedded in paraffin. Consecutive 4-μm sections were cut and 1 slice per 5 mm was examined under a microscope for the pathologic assessment. Histologic diagnosis and staging was based on the latest edition of the World Health Organization classification scheme.[10] The histologic type of adenocarcinoma and the presence of lymphatic involvement were determined using hematoxylin-eosin stained tissue. If the findings could not be determined by hematoxylin-eosin staining alone, immunohistochemical staining was carried out as necessary. An LC ratio was defined as the proportion of LC area relative to the entire tumor. LI and blood vessel invasion were assessed by immunohistochemistry for D2-40, which stains lymphatic ducts, and Van Gieson staining of the elastic fiber of the vessels. LI and blood vessel invasion were determined when spreading through or penetration was detected as an extension of a malignant neoplasm. To evaluate pleural invasion, elastic tissue fibers were subjected to Van Gieson staining. Pleural invasion was determined if cancer cells had invaded beyond the elastic layer, including invasion into the visceral pleural surface, or neighboring organs. Histologic examinations were determined by pathologists from each institution for the purposes of this study.

HRCT

A 16-row multidetector CT was used to obtain chest images. For high-resolution images of the tumors, the following parameters were used: 120 kVp, 200 mA, 1 to 2 mm section thickness, 512 × 512 pixel resolution, 0.5 to 1.0 second scanning time, a high spatial reconstruction algorithm with a 20 cm field of view, and mediastinal (level, 40 Haunsfield unit [HU]; width, 400 HU) and lung (level, −600 HU; width, 1600 HU) window settings. GGO was defined as a misty increase in lung attenuation that did not obscure underlying vascular markings. CT scans were reviewed and tumor sizes determined by radiologists from each institution.

FDG-PET/CT

Patients were instructed to fast for at least 4 hours before intravenous injection of 74 to 370 MBq FDG and then to relax for at least 1 hour before the FDG-PET/CT scan. For imaging, Biograph Sensation 16 (Siemens Healthcare, Erlangen, Germany), Aquiduo (Toshiba Medical Systems Corporation, Tochigi, Japan), or Discovery ST (GE Healthcare, Little Chalfont, United Kingdom) integrated 3-dimensional PET/CT scanners were used. Low-dose nonenhanced CT images of 2 to 4 mm section thickness were taken from the head to the pelvis of each patient. An anthropomorphic body phantom (NEMA NU2-2001; Data Spectrum Corp, Hillsborough, NC) was used to minimize variations in standardized uptake values (SUVs) among the institutions.[11,12] The original SUV_{max} values were determined by radiologists from each institution for the purposes of this study. On FDG-PET/CT images, all lymph nodes in the thorax with FDG uptake no greater than the normal background activity of the mediastinal blood pool—the SUV_{max} of which was <1.5, regardless of size—were considered cN0. A lymph node where the SUV_{max} was ≥1.5 or more was considered "suspicious for malignancy." However, even lymph nodes with high FDG uptake, when they showed higher attenuation than mediastinal structures (great vessels) or benign calcification (central, nodular, diffuse, or popcorn-like), were also considered benign.[13]

Follow-up Evaluation

All patients who underwent lung resections were followed-up from the day after surgery. Postoperative follow-up procedures, including a physical examination and chest radiograph every 3 months and chest and abdominal CT examinations every 6 months, were performed for the first 2 years. Thereafter, a physical examination and chest radiograph were performed every 6 months, and a chest CT examination was performed annually.

Statistical Analyses

Patients with clinical stage IA lung adenocarcinoma were included in the analysis. A Mann-Whitney *U* test was used to compare continuous variables and the χ^2 test or Fisher exact test was used for categorical variables. RFS was defined as the length of time after primary surgical treatment for a cancer ends that the patient survived without any sign or symptom of the cancer. Recurrence was defined as patients having symptoms caused by recurring cancer and suspicious lesions that were diagnosed as recurrent tumors by biopsies. If suspicious lesions were not diagnosed as recurrence, by biopsy, the "recurrence" was comprehensively and clinically defined by radiographic findings, including CT and FDG-PET/CT. RFS and overall survival (OS) curves were calculated using the Kaplan-Meier method. Univariate survival analysis was performed using the log-rank test for comparisons of curves. A Cox regression model was used to calculate *P* values and hazard ratios in the univariate and multivariate analyses. The prognostic analysis was performed during August 2012. All statistical analyses were

performed using EZR (Saitama Medical Centre, Jichi Medical University, Saitama, Japan),[14] which is a graphical user interface for R (The R Foundation for Statistical Computing, version 2.13.0, Vienna, Austria). More precisely, it is a modified version of R Commander (version 1.6-3), which includes statistical functions frequently used in biostatistics.

RESULTS

Clinical Outcomes in Patients With Lung Adenocarcinoma

The median follow-up time was 41.6 months. Lobectomy, segmentectomy, and wedge resection were performed in 375, 97, and 137 patients, respectively. The 30-day mortality rate was 0%. As shown in Table 1, 41 patients (6.7%) had lymph node metastasis in the clinical stage IA lung adenocarcinoma cohort. No significant difference between pN(–) and pN(+) patients was detected in terms of age, sex, and carcinoembryonic antigen value, whereas a marginal difference was seen for tumor size on preoperative high-resolution CT. Regarding the clinical variables, lower GGO ratios and higher SUV_{max} were observed in the N+ group compared with the N– group. In terms of pathologic variables, a lower LC ratio and higher positive rate of LI, blood vessel invasion, and pleural invasion were detected in pN(+) patients. Thirteen of 41 pN(+) patients showed no LI. As shown in Figure 1, *A*, clinical stage IA lung adenocarcinoma patients with lymph node metastasis had a lower RFS rate than those without lymph node metastasis ($P < .001$).

Univariate and Multivariate Analyses of Prognosis According to Pathologic Variables, by Lymph Node Status

Univariate and multivariate analyses of the clinical and pathologic variables were performed to ascertain the most important predictive factor. Univariate analyses were performed on RFS and OS, whereas further analyses, including multivariate analyses, were performed on RFS because OS was more immature than RFS. The pathologic variables included LC ratio, LI status, blood vessel invasion status, pleural invasion status, and lymph node status. For the LC ratio, 30% was used as a threshold because this is the borderline for cT1 N0 M0 lung adenocarcinoma classified as a high- or low-grade malignancy.[2] Univariate analysis revealed that pN(+) patients with LI positive status [LI(+)] had a marginally poorer prognosis ($P = .059$), whereas a lower LC ratio and LI+ status, blood vessel invasion, pleural invasion, or lymph node metastasis was significantly correlated with a poor prognosis in both all patients in this cohort, and in pN(–) patients (Table 2). Additionally, multivariate analysis showed that only LI positive status was a prognostic factor in pN(+) patients ($P = .037$), whereas a lower LC ratio and positive LI status, blood vessel invasion, pleural invasion, or lymph node metastasis were prognostic factors in both all patients and pN(–) patients (Table 3).

TABLE 1. Clinicopathologic findings in patients with clinical stage IA lung adenocarcinoma with or without lymph node metastasis

Finding	Node negative (n = 568)	Node positive (n = 41)	*P* value
Age			
Median	66	65	.33
Interquartile range	60.75-73	56-73	
Sex			
Female	322 (57%)	22 (54%)	.19
Male	246 (43%)	19 (46%)	
CEA			
Median	2.5	3.6	.25
Interquartile range	1.5-3.6	1.1-113.8	
Size*			
Median	2.0	2.2	.060
Interquartile range	1.5-2.4	2.55-4.2	
GGO† ratio			
Median	40	0	<.001
Interquartile range	10-80	0-10	
SUV max			
Median	1.5	3.6	<.001
Interquartile range	0.9-2.6	2.3-4.9	
LC ratio			
Median	50	10	<.001
Interquartile range	10-90	0-20	
Lymphatic invasion			
Negative	507 (89%)	13 (32%)	<.001
Positive	61 (11%)	28 (68%)	
Blood vessel invasion			
Negative	488 (86%)	17 (41%)	<.001
Positive	80 (14%)	24 (59%)	
Pleural invasion			
Negative	515 (91%)	29 (71%)	<.001
Positive	53 (9%)	12 (29%)	

CEA, Carcinoembryonic antigen; *GGO*, ground-glass opacity; *SUV*, standardized uptake value; *LC*, lepidic component. *Tumor size on the high-resolution computed tomography scan. †GGO ratio on the high-resolution computed tomography scan.

Next, we assessed the RFS of pN(–) and pN(+) patients according to their LI status. In both pN(–) and pN(+) patients, RFS rates were lower in LI(+) status compared with LI negative status [LI(–)] ($P < .001$ and $P = .059$) (Figure 1, *B* and *C*). The 3-year RFS and OS rates for each group was as follows: pN(–)/LI(–) 93.4% and 96.7%, pN(–)/LI(+) 70.8% and 85.1%, pN(+)/LI(–) 84.6% and 92.3%, and pN(+)/LI(+) 47.9% and 75.0%, respectively (Table 2 and Figure 1, *B-F*). No significant difference was detected between the pN(+)/LI(–) and pN(–)/LI(+) patients for RFS ($P = .62$; Figure 1, *D*), whereas pN(+)/LI(–) and pN(–)/LI(–) patients, pN(+)/LI(+) and pN(–)/LI(–) patients, and pN(+)/LI(+) and pN(–)/LI(+) patients exhibited significantly different RFS values ($P = .022$, <.001, and .011, respectively).

Clinicopathologic Findings in N+ Patients

In N+ patients, there were no significant differences between the LI(–) and LI(+) groups in terms of age, sex,

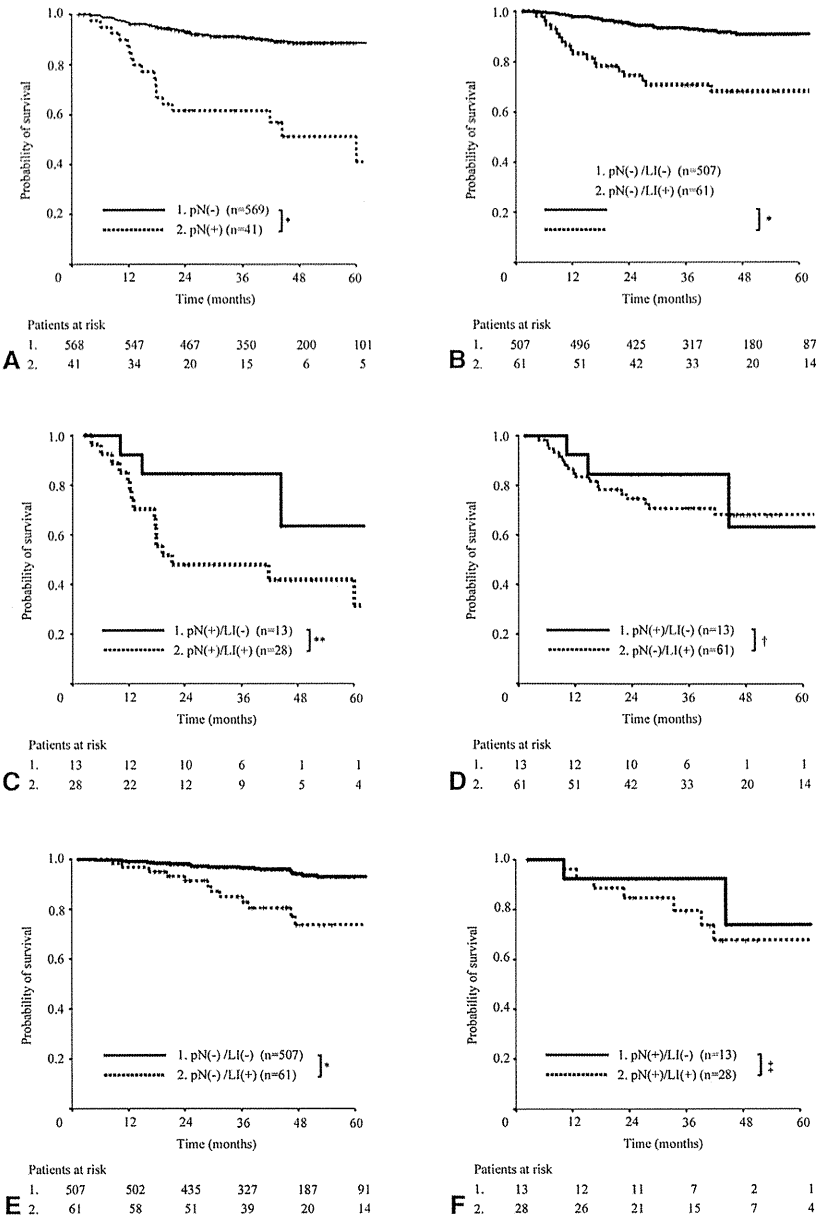

FIGURE 1. Kaplan-Meier recurrence-free survival (A-D) and overall survival (E and F) curves in patients with clinical stage IA lung adenocarcinoma according to pathologic lymph node status and lymph node metastasis and lymphatic invasion (*LI*) status. A, Patients are classified into pathologic lymph node metastasis negative (pN[–]) and positive (pN[+]) groups. B, The pN(–) patients are classified into a lymphatic permeation negative (pN[–]/LI[–]) group and a lymphatic permeation positive (pN[–]LI[+]) group. C, The pN(+) patients are classified into a lymphatic permeation negative (N[+]LI[–]) group and a lymphatic permeation positive (N[+]LI[+]) group. D, Recurrence-free survival curves of pN(+)LI(–) and pN(–)LI(+) patients are shown. E, The pN(–) patients are classified into a pN(–)/LI(–) group and a pN(–)LI(+) group. F, The pN(+) patients are classified into an N(+)LI(–) group and an N(+)LI(+) group. *$P < .001$; **$P = .059$; †$P = .62$; ‡$P = .48$.

carcinoembryonic antigen values, preoperative tumor size, and SUV_{max} values. Regarding pathologic findings, LI status had no association with the LC ratio, blood vessel invasion, and pleural invasion. Additionally, LI status had no correlation with lymph node metastasis status, both single or multiple station metastases (Table 4).

DISCUSSION

In this study, pN(+)/LI(–) patients had a better prognosis than pN(+)/LI(+) patients, whereas there were no significant differences in the RFS between pN(+)/LI(–) and pN(–)/LI(+) clinical stage IA lung adenocarcinoma patients at the participating institutions. LI status, which is

TABLE 2. Univariate log-rank analysis of recurrence-free survival (RFS) and overall survival (OS) according to various factors in patients with lung adenocarcinoma

	All		Node negative		Node positive	
Pathologic variable	**3-y RFS rate (%)**	***P* value**	**3-y RFS rate (%)**	***P* value**	**3-y RFS rate (%)**	***P* value**
LC ratio						
≥30	95.2	<.0001	95.9	<.0001	57.1	.93
<30	78.2		81.4		60.5	
Lymphatic invasion						
Negative	93.1	<.0001	93.4	<.0001	84.6	.059
Positive	63.7		70.8		47.9	
Blood vessel invasion						
Negative	93.1	<.0001	94.3	<.0001	58.8	.93
Positive	63.7		71.0		60.6	
Pleural invasion						
Negative	93.1	<.0001	92.6	<.0001	57.1	.42
Positive	68.6		74.6		65.6	
Lymph node metastasis						
Negative	90.9	<.0001	90.9	—	—	—
Positive	59.9		—		59.9	
	All		**Node negative**		**Node positive**	
	3-y OS rate (%)	***P* value**	**3-y OS rate (%)**	***P* value**	**3-y OS rate (%)**	***P* value**
LC ratio						
≥30	97.0	<.0001	97.3	<.0001	75.0	.76
<30	90.9		92.0		84.5	
Lymphatic invasion						
Negative	96.6	<.0001	96.7	<.0001	92.3	.490
Positive	83.5		85.1		75.0	
Blood vessel invasion						
Negative	96.4	<.0001	96.7	<.0001	88.2	.55
Positive	86.5		88.1		81.0	
Pleural invasion						
Negative	94.9	.0042	95.9	<.0001	100.0	.29
Positive	92.7		91.2		77.3	
Lymph node metastasis						
Negative	95.5	<.0001	95.5	—	—	—
Positive	83.6		—		83.6	

LC, Lepidic component; *RFS*, recurrence-free survival; *OS*, overall survival.

not always positive in N+ patients, is a significant predictive factor in patients with pathologic lymph node metastasis, whereas the lymph node metastasis status is a strong prognostic factor in patients with clinical T1 N0 M0 lung adenocarcinoma.

It is reasonable that lymph node metastasis occurs after cancer cells invade the lymphatic vessels around the tumors; however, 13 of 41 (31.7%) patients with lung adenocarcinoma, whose LI status was negative, exhibited metastasis to regional lymph nodes. One possible explanation is the difficulty in examining all slices of a specimen; some of the slices, including the tumor, could be pathologically assessed. This could be missed if tumors had only slight LI, and the LI status would be determined as negative. Therefore, "no pathologic LI" could either mean no massive LI, just a slight invasion, or it could mean that there was indeed no LI. This is especially the case in pN+ patients, where "no pathologic LI" indicates a slight LI. Slight invasion means the initial period of lymphatic vessel invasion and lymph node metastasis; therefore, patients with slight invasion had a better prognosis than those with massive invasion after complete surgical resection. In pN+ patients the N1 rate was higher in pN(+)/LI(–) patients compared with pN(+)/LI(+) patients, albeit nonsignificantly so. This suggests that pN(+)/LI(–) is indicative of initial lymph node metastasis, as described above.

In pN+ patients, the N2:N1 ratio was higher in pN(+) LI(+) than pN(+)LI(–) patients, although the difference was not statistically significant. The number of pN+ patients was too small to draw any conclusion; however, the tumors that showed massive LI had a higher tendency to progress to N2 disease than LI(–) tumors. Patients with

TABLE 3. Multivariate Cox regression analysis of recurrence-free survival according to various factors

	All		Node negative		Node positive	
Pathologic variables	HR	*P* value	HR	*P* value	HR	*P* value
LC ratio	0.44	.010	0.39	.008	1.7	.62
>30 vs <30	0.23-0.82		0.20-0.78		0.44-6.3	
Lymphatic invasion	2.5	.001	1.9	.045	6.1	.037
Positive vs negative	1.4-4.3		1.0-3.5		1.3-28.7	
Blood vessel invasion	1.8	.037	2.0	.031	0.87	.61
Positive vs negative	1.0-3.1		1.1-3.8		0.31-2.4	
Pleural invasion	1.6	.11	2.1	.024	0.47	.19
Positive vs negative	0.91-2.7		1.1-3.9		0.14-1.5	
Lymph node metastasis	1.9	.032	—*	—*	—*	—*
Positive vs negative	1.1-3.4					

LC, Lepidic component; *HR*, hazard ratio. *Not calculated.

GTS

micrometastatic disease to the lymph nodes have been demonstrated to have a worse prognosis than patients with lymph nodes completely replaced by tumors.[15] This suggests that the continuum from LI to lymph node micrometastasis to lymph node replacement might be more complex than previously believed.

As in previous reports, in all patients, multivariate analysis of RFS revealed a lower LC ratio, positive status of lymph nodes, LI, blood vessel invasion, pleural invasion and were poor prognostic factors as well as N+ status in this study.[16,17] In contrast, all evaluated pathologic variables, except for LI status, did not show potential as predictive factors for patients with lymph node involvement. Although lymphatic metastasis status was a strong prognostic factor, LI status was also a significant predictive factor of prognosis in patients with clinical stage IA lung adenocarcinoma. In pN+ patients, LI status had no association with either the clinical or pathologic findings. Thus, the above findings strongly support the significance of LI status as a predictive factor, particularly in patients whose lymph node status is clinically negative and pathologically positive. That is, poor prognosis should be defined according to not only lymph node status but also LI status. Other unknown factors may more precisely determine the true patient population with a poor prognosis. Although pN+ patients typically receive adjuvant chemotherapy, such patients may be classified into no-adjuvant, mild-adjuvant, and severe-adjuvant groups using several predictive factors, including LI status.

Two previous reports have demonstrated that LI status is a poor prognostic factor in surgically resected non–small cell lung cancer[18,19] and a similar result was shown in pathologic stage I or adenocarcinoma patients. Additionally, LI status has been demonstrated to be a prognostic factor regardless of lymph node status.[18,19] However, these previous studies had some limitations; 1 was the quality of LI status evaluation. LI status was evaluated using D2-40 immunostaining in this study, whereas only some tumors were assessed for LI status using D2-40 in the report[19] and the other did not distinguish LI from blood vessel invasion.[18] Thus, the quality of LI evaluation was higher in our study. Another limitation is heterogeneity of the cohort. The analysis was performed only in pathologic stage I patients in the previous studies to minimize heterogeneity.[18,19] However, that analysis of pathologic stage I patients could not assess LI status in pN+ patients. In our study, we evaluated LI status with little heterogeneity in pN+ patients because we included only clinical stage IA adenocarcinoma patients having little heterogeneity.

The rate of lymph node involvement was 6.7% of clinical stage IA lung adenocarcinoma patients in our study (41 out of 609 cases). PET/CT examination has been shown to provide the most accurate preoperative diagnosis[1,4] and results in appropriate treatment. However, a new diagnostic method is necessary to evaluate more accurately the preoperative status of patients with clinical stage IA adenocarcinoma and pathologic lymph node involvement whose preoperative diagnostic modality included a PET scan.

Few patients had lymph node metastasis in clinical stage IA lung adenocarcinoma, which represents one of the main limitations of this study; only a very small number of patients with lymph node involvement had a negative LI status. This makes it difficult to conclude that the prognosis of pN(+)LI(–) patients is equivalent to that of pN(–) LI(+) patients; however, it cannot be denied that LI status plays an important role in assessing patients with lymph node metastasis. The lack of data about pathologic tumor size or morbidity are also limitations of our study. Another is that detailed numbers on patients who received postoperative chemotherapy were not available. Postoperative chemotherapy was performed when pathologic upstaging or recurrence was detected. Additionally, although the follow-up time was too short to assess OS in this study, the OS curves showed similar tendencies to RFS. Because a previous study reported that RFS could be a surrogate